Groundwater

Review Paper/

Review of Modeling Approaches to Groundwater Flow in Deformed Carbonate Aquifers

by Giacomo Medici[1], Luca Smeraglia[2], Anita Torabi[3,4], and Chartlotte Botter[5]

Abstract

We discuss techniques to represent groundwater flow in carbonate aquifers using the three existing modeling approaches: equivalent porous medium, conduit network, and discrete fracture network. Fractures in faulted stratigraphic successions are characterized by dominant sets of sub-vertical joints. Grid rotation is recommended using the equivalent porous medium to match higher hydraulic conductivity with the dominant orientation of the joints. Modeling carbonate faults with throws greater than approximately 100 m is more challenging. Such faults are characterized by combined conduit-barrier behavior. The barrier behavior can be modeled using the Horizontal Flow Barrier Package with a low-permeability vertical barrier inserted to represent the impediment of horizontal flow in faults characterized by sharp drops of the piezometric surface. Cavities can occur parallel to the strike of normal faults generating channels for the groundwater. In this case, flow models need to account for turbulence using a conduit network approach. Channels need to be embedded in an equivalent porous medium due to cavities a few centimeters large, which are present in carbonate aquifers even in areas characterized by low hydraulic gradients. Discrete fracture network modeling enables representation of individual rock discontinuities in three dimensions. This approach is used in non-heavily karstified aquifers at industrial sites and was recently combined with the equivalent porous medium to simulate diffusivity in the matrix. Following this review, we recommend that the future research combines three practiced modeling approaches: equivalent porous medium, discrete fracture network, and conduit network, in order to capture structural and flow aspects in the modeling of groundwater in carbonate rocks.

[1]G360 Institute for Groundwater Research, College of Engineering and Physical Science, University of Guelph, Guelph, Ontario, N1G 2W1, Canada
[2]Instituto di Geologia Ambientale e Geoingegneria, Consiglio Nazionale delle Ricerche, Piazzale Aldo Moro, 00185, Rome, Italy
[3]Department of Geosciences, University of Oslo, Postboks 1047 Blindern, 0316, Oslo, Norway
[4]Corresponding author: Department of Geosciences, University of Oslo, Postboks 1047 Blindern, 0316 Oslo, Norway; anita.torabi@geo.uio.no
[5]School of Earth and Environment, University of Leeds, Woodhouse Lane, Leeds, West Yorkshire, LS2 9JT, UK

Introduction

Fractured carbonate aquifers, which are subjected to different degrees of karstification, underlie a land area covering approximately 15% of the earth's surface, and they supply drinking water to approximately 25% of the world's population (see Figure 1; Flügel 2013). Approximately 45%, 40%, and 30% of the earth's surface are covered by carbonate rocks in China, northern America, and Europe, respectively (Figure 1; Worthington and Ford 2009; Ford and Williams 2013; Hartmann et al. 2014a, 2014b). In these areas, stress on groundwater resources is much higher due to high population densities, which necessitate intense industrial and agricultural activities. Thus, a range of pollutants such as nitrate, sulfate, chloride, pathogens, toxic organic compounds released by mineral fertilizers and pesticides can reach the saturated parts of these aquifers in regions, which are devolved to industry and agriculture (Bales et al. 1989; Göppert

and Goldscheider 2008; Mahler and Garner 2009; Petitta et al. 2009, 2018; Musgrove et al. 2014; Zhang et al. 2019; Medici et al. 2020). Additionally, carbonate aquifers represent the principal source of water for major capital cities such as Doha, Beijing, London, Rome, and Vienna (Maloszewski et al. 2002; Worthington and Gunn 2009; Ford and Williams 2013; Hartmann et al. 2014a, 2014b; Worthington 2015). Hence, the exponential geo-modeling advance of the last 30 years has presented new solutions for the representation of groundwater flow in aquifers of carbonate origin in response to the social and economic importance of these geological media (Shoemaker et al. 2008; Reimann and Hill 2009; Hill et al. 2010; Gallegos et al. 2013; Saller et al. 2013; Hartmann et al. 2014a; Sullivan et al. 2019). However, new modeling advances should be integrated with traditional techniques for rigorous representation of fluid flow in a three-dimensional (3D) geological domain. Further, all modeling techniques should honor the corresponding tectonic settings.

Within carbonate aquifers, fluid flow is primarily controlled by bedding planes reactivated by the tectonic stress (Tanner 1989; Ritzi and Andolsek 1992; Bidaux and Drogue 1993; Odling et al. 1999; Bauer et al. 2016; Medici et al. 2016, 2019a, 2019c). Groundwater flow is particularly rapid in areas of intense fracturing such as damage zones of normal faults and thrusts and intensely fractured fold hinges and limbs. In these settings, karstification can be much more intense, where conduits characterized by turbulent flow occur in the subsurface (Shoemaker et al. 2008; Göppert et al. 2011; Amoruso et al. 2013; Chen and Goldscheider 2014; Medici et al. 2019b). Such conduits have been detected by televiewer logging and persist in carbonate aquifers at different depths ($\sim$10–200 m) below the water table (Goldscheider and Drew 2014; Medici et al. 2019a). Hence, carbonate aquifers are characterized by a complex 3D pattern of bedding planes, tectonic fractures, and karst conduits. Currently, three different approaches are used to model fluid flow in this structural complexity: equivalent porous medium (EPM), conduit network (CN), and discrete fracture network (DFN) (Selroos et al. 2002). The simplest modeling approach is EPM. This method treats the fractured rock with channels as an EPM, using bulk properties instead of the physical characteristics of the matrix, individual fractures and conduits (Yager et al. 2009). By contrast, the DFN and CN approaches represent groundwater flow in individual fractures and channels, respectively (Shoemaker et al. 2008; Parker et al. 2019). These approaches are impaired, as they overlook the structural features and their effects on the fluid flow in different tectonic settings. As contaminants are transported at higher rates in rock discontinuities of primary tectonic origin, much more attention is needed on the structural geology aspect of the conceptual model than merely the numerical components of groundwater flow models in carbonate aquifers (Odling et al. 1999; Aydin 2000; Lemieux et al. 2006; Lacombe and Burton 2010; Wang et al. 2017).

To account for both recent advances in modeling fluid flow in the subsurface and the brittle structural behavior of carbonate rocks, a first review that combines the two aspects is here proposed. Fault geometry and architectural studies by structural geologists concerning the potential influence of faults on fluid flow are mostly based on outcrop observations and geophysical data from petroleum reservoirs (see Faulkner et al. 2010, and Solum and Huisman 2016 for reviews). Bense et al. (2013) reviewed all the experimental methods of hydraulic investigation of fault zones. Fiorillo et al. (2015) studied the recession of springs in karst aquifers worldwide from a hydrological point of view. A number of review papers focus on the hydraulic behavior of fractured and karst aquifers in specific regions (e.g., Ghasemizadeh et al. 2012; Guo et al. 2013).

Other recent reviews focus on the links between paleoclimate and ecosystem and the hydrogeology of carbonate aquifers (Goldscheider 2012; Hartmann and Baker 2017). Applicability of karst aquifers to low and medium enthalpy geothermal resources were revised by Goldscheider et al. (2010), Hartmann et al. (2014a), and Kalhor et al. (2019) that provide a review of the most recent modeling approaches to karst hydrology. However, these works do not relate modeling approaches to the tectonic structures and exclusively discuss the use of EPM and CN methodologies.

Similar to other authors, we consider fractured carbonate aquifers strongly anisotropic and heterogeneous due to the coupling of pervasive fracturing and karstification (Worthington 1991; West and Odling 2007; Goldscheider and Drew 2014; Hartmann et al. 2014a; Borović et al. 2019). However, the majority of groundwater flow models only account for the vertical flow anisotropy (K_h/K_v), which is in a wide range ($\sim$10^2–10^3) in karst environments (Neymeyer et al. 2007; Odling et al. 2013; Goldscheider and Drew 2014; Zuffianò et al. 2016).

Anticlines, synclines, and areas affected by vertical lithosphere uplifts are characterized by dominant sets of sub-vertical joints (Odling et al. 1999; Gillespie et al. 2001; Billi 2005; Carminati et al. 2010; Tavani et al. 2015). These structural patterns can induce horizontal flow anisotropies that influence the direction and rate of contaminant dispersal in the subsurface. Shape and velocities of plumes are influenced by preferential orientation of tectonic fractures in geological porous media (Odling and Roden 1997; Berkowitz 2002). This horizontal flow anisotropy (K_y/K_x) also finds practical application in the definition of the source protection areas in karst aquifers. In fact, backwards particle tracking from abstraction wells is influenced by the introduction of horizontal flow anisotropies in 3D groundwater flow models (Pollock 1994).

Extensional tectonic settings, fold and thrust belts, and vertically uplifted areas are characterized by normal faults that accommodate local or crustal scale extension (Jolivet and Faccenna 2000; Billi 2005; Carminati et al. 2009). Hence, conceptual and technical details on modeling groundwater flow in normal faults are added in this research.
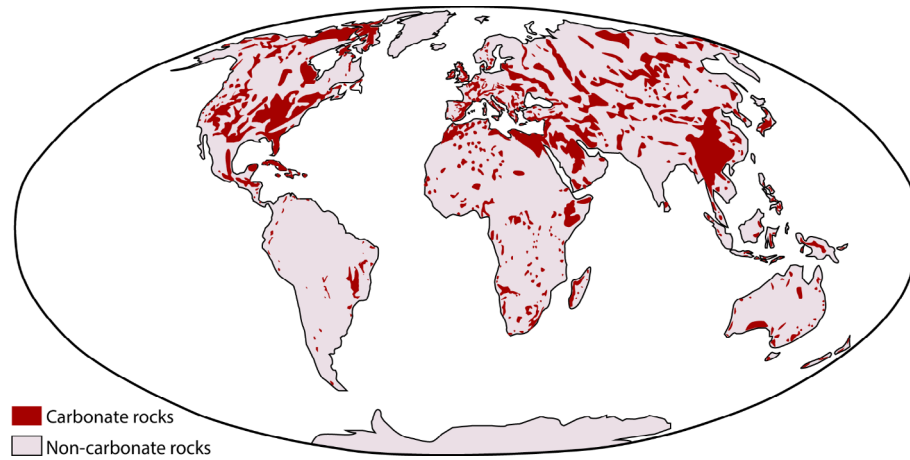
Figure 1. World map with outcrops of carbonate rocks (from Flügel 2013).

In summary, utilizing the EPM and DFN methods, this review links groundwater flow modeling to the structural pattern in the saturated zone of carbonate aquifer types. Specific research objectives are: (1) to provide guidelines to model groundwater flow in the subsurface in the presence of normal faults, folds, thrusts, and uplift-generated joints; (2) to relate modeling strategy to the existing flow modeling approaches in geological media; and (3) to identify future research scenarios on numerical modeling in carbonate aquifers.
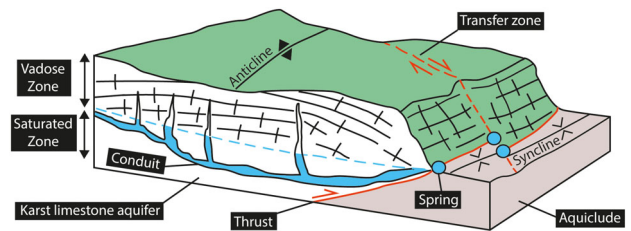

Figure 2. Three-dimensional hydro-structural model of thrusts (modified from Goldscheider and Drew 2014).

Hydrogeology of Tectonic Structures

The 3D network of rock discontinuities and karst conduits in faulted and unfaulted areas are described based on structural, geo-morphological surveys and speleological observations. This description, coupled with experimental evidences of the impact of thrusts, folds, and normal faults on fluid flow, represents a primary step before moving toward numerical modeling. Flow anisotropies are the result of dominant sets of tectonic fractures in carbonates aquifers (Odling et al. 1999, 2013; Billi 2005; Hartmann et al. 2007; Agosta et al. 2010; Korneva et al. 2014). However, flow heterogeneities are represented by systems of caves and cavities that due to relatively large aperture ($\sim 10^{-2} - 10^{0}$ m) are characterized by high-flow velocities and turbulent flow (Bauer et al. 2003; Shoemaker et al. 2008; Gallegos et al. 2013; Masciopinto and Palmiotta 2013; Saller et al. 2013; Sauro et al. 2013; Medici et al. 2019a, 2019b). The following section describes the relation between flow anisotropies, heterogeneities, and tectonic structures.

Fold and Thrust Belts

Folds can form in association with detachments, as well as propagating and bending faults (e.g., Allmendinger 1998; Carminati et al. 2010). Thrust faults and folds (anticlines and synclines) observed at a much finer scale ($\sim 10^{0} - 10^{1}$ m) appear heavily fractured and karstified in quarries and road cuts (Billi et al. 2007; Pepe and Parise 2014; Tavani et al. 2015; Bauer et al. 2016; Medici

et al. 2019b; Smeraglia et al. 2020). Hence, understanding preferential orientation of fractures as conduits is of paramount importance to model groundwater flow in the subsurface in mountain belts (Petitta and Tallini 2002; Falcone et al. 2008; Göppert et al. 2011; Bakalowicz 2015).

Thrusts that displace carbonate sedimentary successions are typically characterized by an alignment of springs (Figure 2). Troughs, where the springs are located, are used to map thrusts in vegetated areas in a mountain range. The alignments of springs arise from either presence of relatively impermeable marly lithologies at footwall blocks or development of low-permeability cores in the thrust plane (Boni et al. 1986; Cosentino et al. 2010; Giacopetti et al. 2017).

Springs are connected to a network of caves and cavities in the subsurface (Scozzafava and Tallini 2001; Sauro et al. 2013; Goldscheider and Drew 2014; Giacopetti et al. 2017). Such conduits are approximately 0.1–5 m large according to outcrop and speleological observations and tend to be orthogonal to the thrust faults (Figure 2). This orientation is attributed to the development of valleys that perpendicularly cut the compressional front. Most of these valleys are related to strike-slip tear faults that divide sectors of thrusts characterized by different displacements (Figure 2b; Boyer and Elliot 1982; Miccadei et al. 2011). Here, relatively high groundwater flow velocities and turbulence occurs. In fact, high turbidity of springs associated with major thrusts is due to turbulent currents that
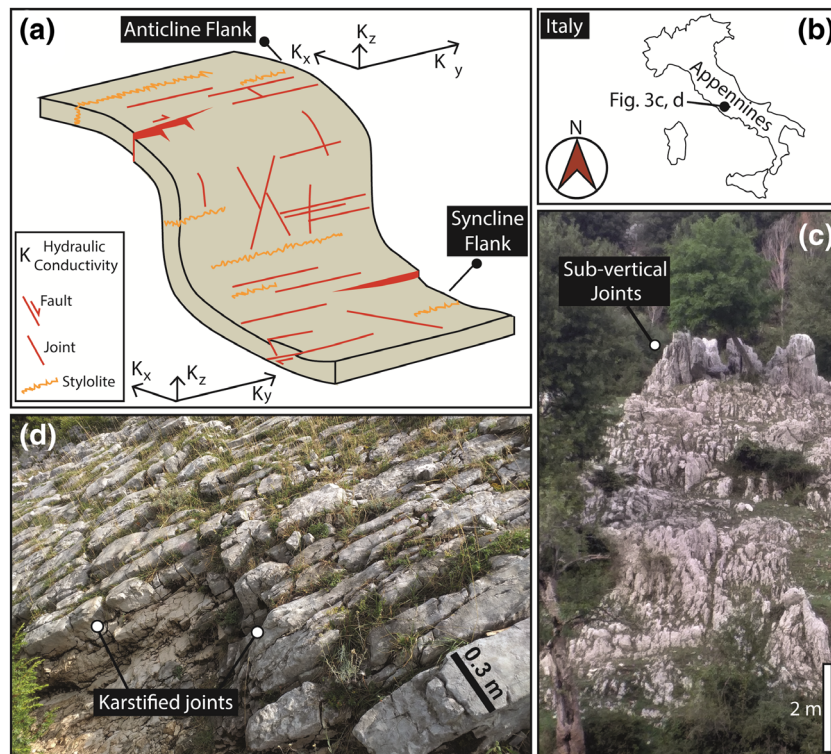
Figure 3. Hydrogeology versus folds: (a) hydro-structural model of anticlines and synclines (modified from Tavani et al. 2015); (b) map of Italy with location of outcrops in (c) and (d); (c) sub-vertical fold-related fractures, Vivaro Romano (Latium, Central Italy); (d) karstification of sub-vertical fold-related fractures, Vivaro Romano (Latium, Central Italy).

resuspend solid particles (Angelini and Dragoni 1997; Amraoui et al. 2003).

Rock discontinuities in anticline and syncline structures in fold and thrust belts are dominated by open fractures oriented perpendicular to bedding surfaces and striking parallel and oblique to fold axis (see Figure 3a and d). These high angle rock discontinuities are hydraulically conductive (Figure 3c and d). Minor faults (throw $< \sim 10$ m) also form in the fold hinge zone. Stylolites, which represent typical fluid flow barriers, are pervasively oriented sub-parallel to fold hinge (Figure 3a; Tondi et al. 2006; Carminati et al. 2010; Tavani et al. 2015). As a consequence, hydraulic conductivity tends to be higher parallel to the fold axis (Figure 3a). The orientation of folds axis can be considered constant at the scale of approximately 0.5–5 km according to geological maps in folded areas (Santantonio et al. 2017; Mercuri et al. 2020). At this spatial scale of a few kilometers, contaminant plumes are constrained by geophysical monitoring at industrial field sites (Chapman and Parker 2005; Parker et al. 2008). Hence, the hydro-mechanical anisotropy of anticlines and synclines may influence spatial extension and dispersal rate of these plumes in the subsurface.

However, in mountain belts, anticlines and synclines play a different hydrogeological role. Typically, anticlines represent topographic highs that approximately coincide with groundwater divides (Cosentino et al. 2010; Lauber and Goldscheider 2014). Synclines more commonly represent valleys, and therefore, hydraulic gradients and

modulus of the groundwater flow vector are elevated due to the steep topography (Goldscheider 2005; Worthington and Ford 2009; Chen and Goldscheider 2014; Lauber and Goldscheider 2014). Here, rapid groundwater flow occurs and facilitates rock dissolution with vigorous and continuous refreshment of groundwater, which is less saturated in calcite, aragonite, and dolomite. Thus, karstification occurs and tends to be sub-parallel to the syncline axis (Worthington 1991; Goldscheider 2005). The maximum hydraulic conductivity and flow vectors are approximately sub-parallel to the preferential orientation of open fractures according to hydro-mechanical models (Figure 3a; Carminati et al. 2010; Evans and Fischer 2012; Chen and Goldscheider 2014; Tavani et al. 2015). The coupling between groundwater flow direction and its high rate in the valleys explains the presence of karst conduits parallel to the syncline axis.

Conduits have been detected parallel to the syncline structures in the Canadian Rocky Mountains and the Austrian and German Alps (Worthington 1991; Goldscheider 2005; Gremaud et al. 2009; Chen and Goldscheider 2014). Here, tracer tests indicate high-flow velocities up to 200 m/h in valleys where synclines are mapped (Worthington 1991; Göppert and Goldscheider 2008).

Unfaulted Uplifted Areas

Areas of the world characterized by sub-horizontal layers ($<5°$) and absence of compressional tectonic structures are deformed by gentle flexuring of geological strata due to vertical uplifts of the lithosphere (Carminati
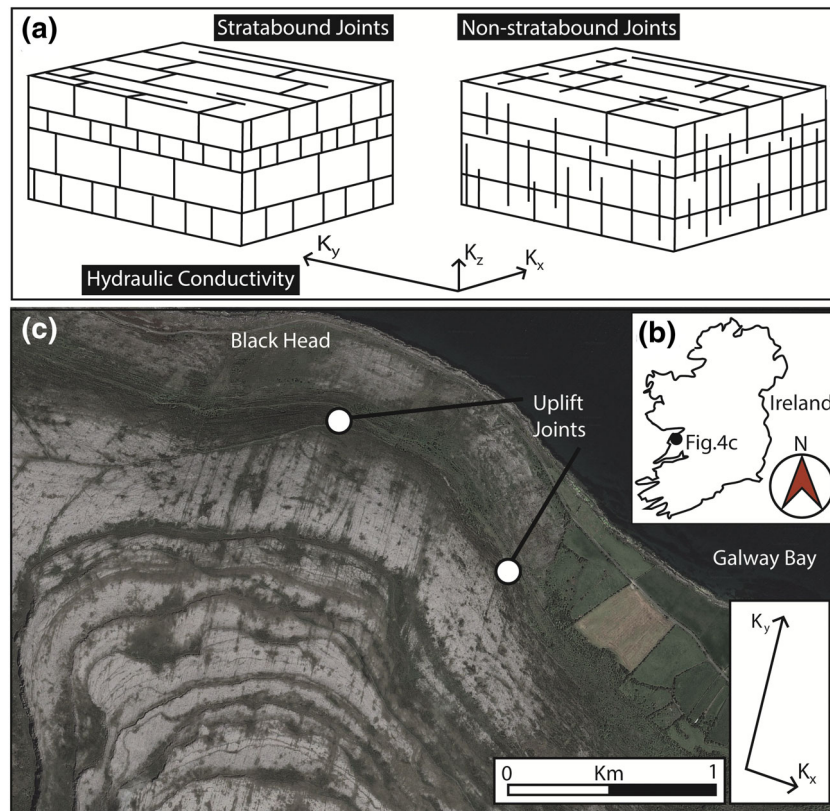
Figure 4. Hydrogeological behavior of uplift-generated joints: (a) hydro-structural model of stratabound and non-stratabound joints (modified from Odling et al. 1999); (b) map of Ireland with location aerial photograph in (c); (c) Google Earth aerial photograph showing orientation principal set of joints in the Carboniferous Limestone of Burren at Black Head, western Ireland (after Gillespie et al. 2001).

et al. 2009). This structural scenario is observed in Cretaceous limestones of Sicily and Apulia, Carboniferous limestones of west Ireland and northern England, Cretaceous limestones of southern France, and Silurian dolostone of Ontario (Allen et al. 1997; Gillespie et al. 2001; Billi 2005; Odonne et al. 2007; Parker et al. 2019). Here, the fracturing pattern away from fault zones is characterized by sub-vertical and orthogonal joint sets that occur either as stratabound or nonstratabound systems (Figure 4a). Such joints are in both cases characterized by a preferential orientation (Figure 4a–c). Outcrops also show evident enlargement of these discontinuities by groundwater dissolution (Odling et al. 1999; Gillespie et al. 2001; Billi 2005; Odonne et al. 2007; Murphy and Everett 2013; Goldscheider and Drew 2014). Fluid logs and dilution tests reveal how bedding plane fractures represent the principal flow pathways. However, hydraulic connection between bedding plane discontinuities is established by sub-vertical joints (Hartmann et al. 2007; West and Odling 2007). Pumping tests carried out with observation wells with an approximately 10 m spacing indicate an elliptical drawdown with major axis elongated in the dominant orientation of sub-vertical joints in the Carboniferous limestone of western Ireland and Great Britain and the Cretaceous limestone of southern France (Allen et al. 1997; Barrash and Dougherty 1997; Wang et al. 2016). A 40 years groundwater monitoring

with high-resolution depth-discrete multi-level sampling systems shows a clearly delineated bedrock plume. The plume shape is influenced by orientation of bedding plane fractures and sub-vertical joints in the Silurian Dolostone of Ontario in the Guelph Municipality (Parker et al. 2019).

Thus, the presence of a principal set of sub-vertical flowing joints induces horizontal flow anisotropies in fractured rock masses. The horizontal hydraulic conductivity tends to be higher parallel to the principal trend of joints in unfaulted areas as illustrated in the hydro-mechanical model in Figure 4a.

High Angle Faults

Normal and strike slip faults that develop in low-porosity carbonates are characterized by fault cores of cataclasites and clay smears and areas of intense fracturing defined as damage zones (see conceptual model Figure 5a). Low-displacement (throw < ~100 m) faults tend to primarily develop damage zones that are dominated by highly conductive open fractures (Figure 5; Caine et al. 1996; Bauer et al. 2016; Torabi et al. 2019b). Indeed, the fault throw versus damage zone width curve flattens for throw values greater than approximately 100 m in carbonate rocks. Fault cores become progressively more important with the rising of throw (Figures 5, and 6a–d; Agosta and Kirschner 2003;
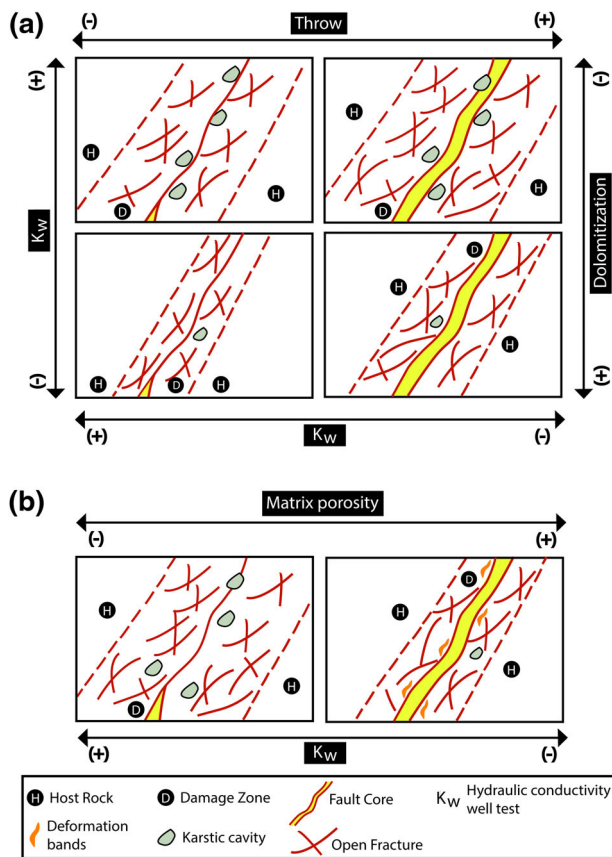
Figure 5. Hydro-structural conceptual models of normal faults in limestone and dolostone: (a) dolomitization versus throw versus hydraulic conductivity (modified from Caine et al. 1996 and Bauer et al. 2016); (b) matrix porosity versus hydraulic conductivity (after Tondi et al. 2006 and Torabi et al. 2019b).

Torabi et al. 2019a, 2019b). Cataclastic fault cores are characterized by low-porosity fine-grained matrix generated by processes such as grain fracturing, chipping, and further abrasion, which reduce the grain size of the host rock. Mature fault zones show a core up to several meters thick, which is typically cohesive due to mechanical compaction and/or cementation (Figure 6d; Faulkner et al. 2010). This structural feature is capable to reduce the hydraulic conductivity of the fault, at least in the direction perpendicular to the fault plane (Figure 5; Aldrick 1978; Celico et al. 2006; Petrella et al. 2009). The conceptual scheme in Figure 5a has been developed by studying the architecture of normal and transtesional faults in lithoid and low-porosity carbonate rocks of Triassic age in the Austrian Alps (Bauer et al. 2016).

Damage zone of faults are characterized by fractures, veins, and deformation bands depending on the initial porosity of the carbonate rock under deformation. Porous carbonate rocks are less prone to fracturing and tend to primary develop low-permeability cores with increasing fault throw, while the damage zone is less fractured than that of faults developed within low-porosity carbonates (Antonellini et al. 2014; Torabi et al. 2019a, 2019b, 2020).

Fault cores within porous carbonates are characterized by deformation bands showing pore collapse and grain compactions (Tondi et al. 2006). Thus for the same value of throw, the core is more developed than the damage zone in faults that displace porous carbonate rocks with respect to the lithoid and low-porosity ones (see conceptual scheme in Figure 5b; Tondi et al. 2006; Torabi et al. 2019a).

Veins and deformation bands represent fluid flow barriers (Figure 5b; Billi et al. 2003; Agosta and Aydin 2006; Micarelli et al. 2006; Cilona et al. 2012; Antonellini et al. 2014; Kaminskaite et al. 2019). Fractures create high-permeability pathways within the damage zone allowing the vertical and lateral fluid movements along the fault zone (Caine et al. 1996). Notably, large-displacement (throw > ~100 m) normal faults in limestones and dolostones are also characterized by up to 40° change of trend in geological maps. This structural characteristic is related to the linkage of neighboring and nonparallel normal faults that occur in carbonate rocks at a variety of scales (Dawers and Anders 1995; Mercuri et al. 2020). From a geomorphological point of view, normal faults are frequently associated with cavities, karsts, and dolines with principal axes sub-parallel to the fault plane in carbonate rocks (Kresic 1995; Göppert et al. 2011; Pepe and Parise 2014).

Cavities with rounded and angular shapes are recognized in outcrop in fractured limestone and dolostone (Figure 7a–e). These structures typically represent fault jogs (Figure 7c) and bedding plane discontinuities (Figures 6e) enlarged by groundwater dissolution in fault zones (Woodcock and Mort 2008; Sauro et al. 2013). Intensively karstified jogs and bedding plane discontinuities occur associated with undulation of the normal fault plane parallel to the strike of the fault planes. Jogs with cavities and caves are also localized in small-scale (~1–10 m in lengths) releasing band structures related to change in the strike direction of transtensional faults (Murphy and Burgess 2006; Billi et al. 2007; Sauro et al. 2013; Bauer et al. 2016; Medici et al. 2019b).

Caves and cavities tend to be larger in limestone compared to dolostones, which are less prone to dissolution (Murphy 2000; Farrant and Cooper 2008; Bauer et al. 2016). Normal faults of similar throw in limestones tend to be more permeable than those in dolostones (see Figure 5a). However, alignment of springs is common in normal faults in carbonate rocks, subjected to different degrees of dolomitazation (Kresic 1995; Caine et al. 1996; Agosta and Kirschner 2003; Falcone et al. 2008; Gremaud et al. 2009; Lauber and Goldscheider 2014; Pepe and Parise 2014; Bauer et al. 2016).

Single-borehole pumping tests that intercept the damage zone of normal and strike slip faults confirm all the above described structural, geomorphological, and speleological indicators. Such tectonic structures are characterized by permeabilities up to two order of magnitude higher than the host rock in fractured carbonates (Aldrick 1978; Allen et al. 1997; Medici et al. 2019b). However, evidence of hydraulic barrier behavior across normal faults
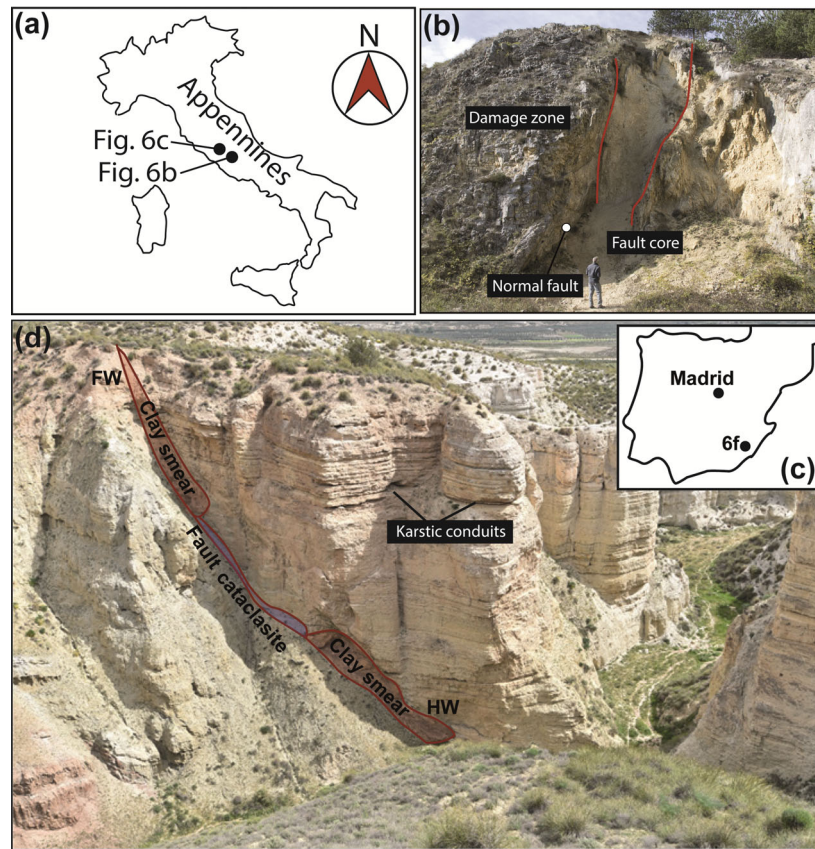
Figure 6. Normal faults: (a) map of Italy showing location of outcrops in (b) and (c); (b) fault in Mesozoic limestones showing the fractured damage zone and the cataclastic fault core, Venere Fault (Central Apennines, Italy); (c) map of Spain showing the location of the outcrop in (d); (d) the Basa Fault in southern Spain displacing carbonates of Miocene age; clay rich and cataclastic core and karstic conduits in the hanging wall block (interpretation from Torabi et al. 2020).

is more common in relatively high-displacement (throw > ~100 m) faults due to presence of continuous, relatively thick, and low permeable cataclastic and clay-rich fault cores (Figures 5a and 6b; Caine et al. 1996; Billi et al. 2003; Micarelli et al. 2006; Antonellini et al. 2008; Faulkner et al. 2010; Smeraglia et al. 2016a, 2016b; Ortiz et al. 2018; Torabi et al. 2019a, 2019b). Large-displacement normal faults in southern France and central Italy displacing Meso-Cenozoic limestones compartmentalize aquifers (Celico et al. 2006; Bucci et al. 2014). In fact, moving from the hanging wall to the footwall the piezometric surface rapidly drops. The well test-scale hydraulic conductivity of these large-displacement normal faults is reduced in the case of screens intercepting low-permeability cataclastic core (Figure 5b; Dausse et al. 2019).

Applications of Modeling Approaches

Groundwater flow and solute contaminant transport occur at much higher rates along bedding planes, joints, and damage zone of low-porosity carbonates (Berkowitz 2002; Guo et al. 2019). Hence, the modeling strategy must be arranged accounting for the structural setting, which controls the pattern of the rock discontinuities. A range of practical solutions is proposed below to

guide geo-modelers toward reliable representation of fluid flow in the subsurface in limestone and dolostone aquifers. Note that the proposed solutions refer to the three different methods used to model fluid flow in fractured and karst aquifers: (1) EPM, (2) CN, and (3) DFNs (see conceptual scheme in Figure 8).

Equivalent Porous Medium

Tectonic fractures typically show a principal orientation in the hinterland of fold and thrust belts (e.g., Figures 2 and 3) as well as in relatively undeformed areas (e.g., Figure 4). The dominant orientation of open fractures is sub-parallel to the axes of anticlines and synclines in mountain ranges (Figure 3a; Carminati et al. 2010; Evans and Fischer 2012; Tavani et al. 2015). Joints are also characterized in unfaulted areas by orthogonal sets of high ($70°-90°$) angle fractures with a more persistent set (Figure 4a–c; Odling et al. 1999; Gillespie et al. 2001; Billi 2005; Odonne et al. 2007). Rotation of grid (see Figure 9a) axes allows assigning higher hydraulic conductivity values in the direction of preferential orientation of open fractures in EPM flow models based on the Darcy's law. Note that, for details on coordinate transforms and parameters relative to the Darcy's equation that describes laminar flow in anisotropic media, the reader is referred to Harbaugh 2005.
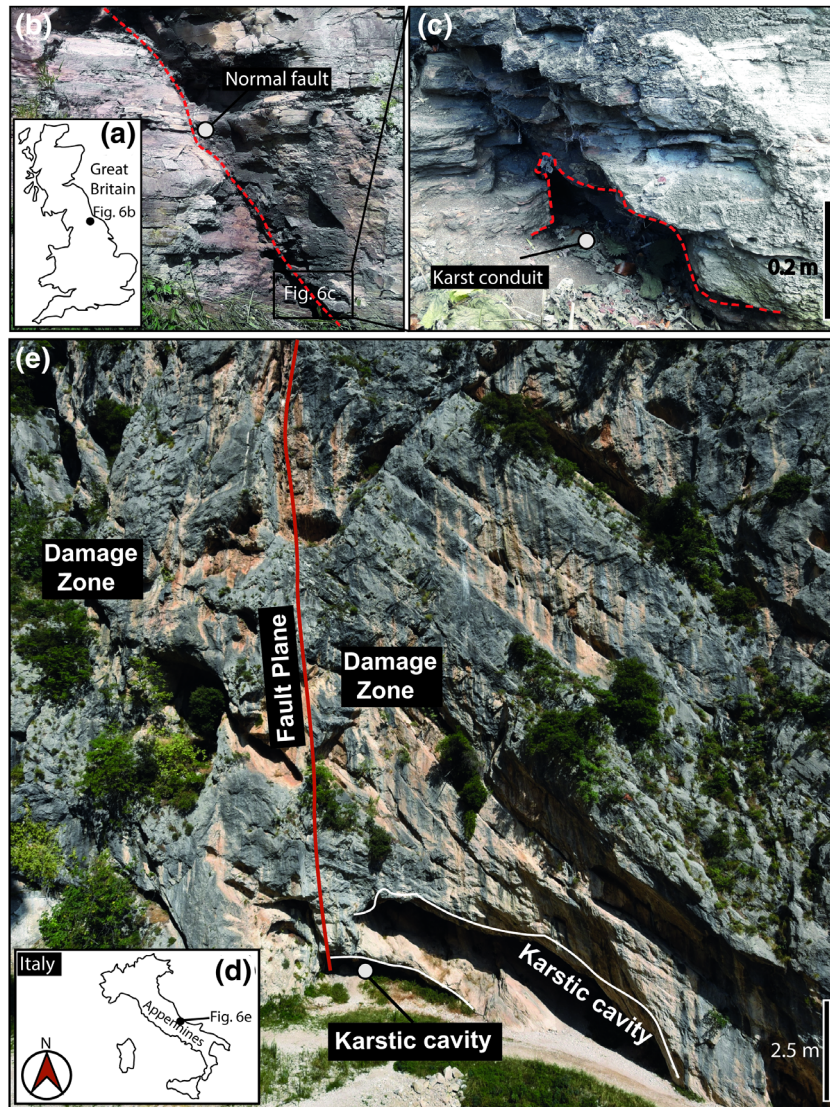
Figure 7. Normal and strike-slip faults: (a) map of Great Britain with location of the outcrop in (b); (b) normal fault in the Permian Dolomitic Limestone of Leeds, Yorkshire (from Medici et al. 2019b); (c) detail of karstic cavity related to the normal fault in Leeds, Yorkshire; (d) map of Italy showing the location of studied outcrop in (e); (e) karstic cavities in the damage zone of strike-slip faults in the Miocene deposits of the Majella Massif, Fara San Martino, Central Italy.

A previous study found better calibration of steady state models in Permian dolomitic limestones of Great Britain by introducing a hydraulic conductivity two times higher in the direction of the dominant set of joints (Medici et al. 2019b). Other authors support the latter solution used in the Permian dolomitic limestones of Great Britain in other carbonate aquifers arranged in either stratabound or nonstratabound joint system with a set of sub-vertical fractures that is dominant in the studied outcrops (Odling et al. 1999; Lemieux et al. 2006). Note that, matching horizontal grid axis with the direction of maximum hydraulic conductivity brings a more detailed representation of capture zones around abstraction wells and plume dispersal when moving from groundwater flow to transport modeling (Pollock 1994; Berkowitz 2002).

By contrast, rotation of grids to introduce horizontal anisotropies is not adequate for normal faults (see conceptual model Figure 9a and b). The direction of such tectonic structures is less spatially consistent than fold axis in thrust belts at the scale of a few to up to several kilometers. This structural pattern is related to linkage of non-subparallel normal faults (Soliva and Benedicto 2004; Mercuri et al. 2020). Similarly, normal faults show variation of up to approximately 40° in their trends in areas where uplift-generated joints are mapped in fractured limestones (Gillespie et al. 2001). Hence, rotation of grids (Figure 9) must be defined with reference to folds and uplift-related joints in the co-presence of normal faults.

Carbonate aquifers are primarily characterized by high conductive flow pathways in both faulted and unfaulted areas. In contrast, a range of high-angle (60°–90°) centimeter to meter scale tectonic structures such as cataclasites, veins, and deformation bands
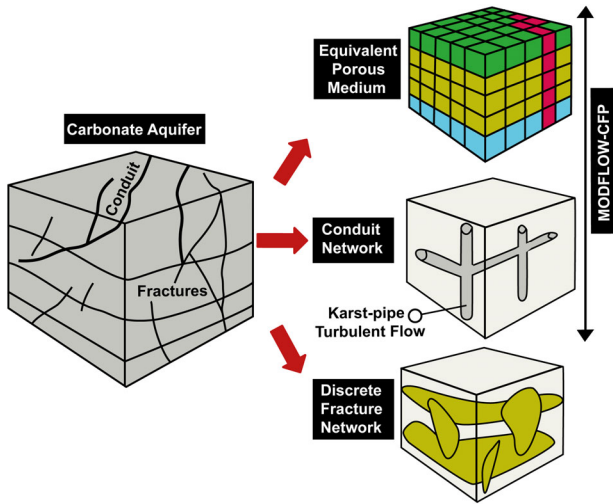
Figure 8. Conceptual model of a carbonate aquifer and the EPM, CN, and DFN approaches to flow modeling (modified from Selroos et al. 2002).

occurs around faults (Billi et al. 2003; Agosta and Aydin 2006; Micarelli et al. 2006; Cilona et al. 2012; Antonellini et al. 2014; Smeraglia et al. 2018; Kaminskaite et al. 2019). This variety of flow barriers and baffles reduces the field and regional-scale permeability in several study cases. This permeability reduction is related to the continuity of cataclastic fault cores in large (throw > ~100 m) scale normal faults in carbonate aquifers (Figure 5; Aldrick 1978; Petrella et al. 2009). The reduced hydraulic conductivity is related to the thick core of normal and strike-slip faults that act as partial barriers (Hsieh and Freckleton 1993; Caine et al. 1996).

To account for this, the USGS introduced the MODFLOW-2005 Horizontal Flow Barrier (HFB) Package to insert in the cells of the EPM (see Figure 9b; Hsieh and Freckleton 1993). A thin and vertical barrier of defined low hydraulic conductivity is inserted to represent the impediment of horizontal groundwater flow. The key assumption underlying the HFB Package is that the width of the fault core is negligibly small compared to the horizontal dimensions of the cells in the grid (Hsieh and Freckleton 1993). To apply this numerical solution, average thickness of the fault core must be extrapolated from outcrop measurements. Furthermore, permeability tests on plugs of cataclastic samples provide the hydraulic conductivity of the fault core (Fisher and Knipe 2001; Al-Hinai et al. 2008; Trippetta et al. 2017; Fisher et al. 2018; Kaminskaite et al. 2019).

Some authors insert the HFB package in axes of gentle anticlines in fractured aquifers (Ely et al. 2011, 2014). In fact, such fold structures are characterized by sub-vertical axial planes. Bedding planes represent the principal flow pathways in fractured geological porous media (Tsang and Witherspoon 1983; Allen et al. 1997; Paillet 1998; Odling et al. 1999, 2013; Jourde et al. 2002, 2007; West and Odling 2007; Medici et al. 2016, 2018, 2019a). Undulation of bedding discontinuities causes reduction of groundwater flow

perpendicular to the fold axis and compartmentalizes aquifers as demonstrated by hydrochemical analyses (Douglas et al. 2007). However, grid rotation also allows increasing the hydraulic conductivity parallel to the fold axes due to preferential orientation of fold-related joints (Figure 3a). The latter solution seems to be a better strategy, as it accounts for both (1) hydraulic conductivity enhancement in the direction parallel to the fold axis due to preferential orientation of joints, and (2) hydraulic conductivity reduction perpendicular to the axis due to folding of the bedding planes (Figure 9).

Conduit Network

Fractured limestones and dolostones are subjected to karstification and hence enlargement of rock discontinuities by dissolution of calcite, dolomite, and aragonite. Dominance of turbulent flow is likely to occur in carbonate aquifers in areas subjected to elevated flow rates (Shoemaker et al. 2008; Worthington and Ford 2009; Reimann et al. 2011; Hartmann et al. 2014a; Assari and Mohammadi 2017; Medici et al. 2019a, 2019b). Intense groundwater flow occurs around normal and strike-slip faults and thrusts due to the high density of the fracture network. Here, the rapidity of flow enhances dissolution of carbonate minerals (Maurice et al. 2006; Worthington and Ford 2009; Worthington and Gunn 2009). Synclines are also exposed to intense karstification, that is, formation of steep valleys that drive rapid groundwater flow in the subsurface (Goldscheider 2005; Göppert et al. 2011; Chen and Goldscheider 2014). As a consequence of this, caves and cavities tend to develop parallel to the strike of normal and transcurrent faults and syncline axis (Figure 7c–e; Torabi et al. 2019b). The coupling of conduits and high hydraulic gradients in these three tectonic structures causes local occurrence of turbulent flow.

Discrete karst conduits must be embedded in the EPM that accounts for laminar flow in the fractured carbonate rock (Figure 9c). The drainage network of the karstic features must be defined by outcrop, speleological, and tracer test observations to apply this strategy (Chen and Goldscheider 2014; Medici et al. 2019b). Equations 1 and 2 derived from the Darcy-Weisbach formula are used in specific cells to describe laminar (Q_l) and turbulent (Q_t) flow, in cavities and caves of approximate pipe-shape, respectively (Figure 8; see Shoemaker et al. 2008 for mathematical details).

$$Q_l = -\frac{d^4 \pi g \Delta h}{128 k \Delta l \tau} \tag{1}$$

$$Q_t = -\frac{\Delta h}{|\Delta h|} \sqrt{\frac{|\Delta h| \, g d^5 \pi^2}{2 \Delta l \tau}} \log \frac{2.5 k \Delta l}{\sqrt[4]{\frac{2|\Delta h| g d^3}{\Delta l \tau}}} + \frac{r}{3.71 d} \tag{2}$$

In the equations above, d (L) is the pipe diameter, τ (−) is the pipe tortuosity, r (L) is the average asperity height of the pipe walls, k (L²/T) is the kinematic viscosity, g (LT^{-2}) is the gravitational acceleration constant, Δl (L) is pipe length, and Δh (L) is the
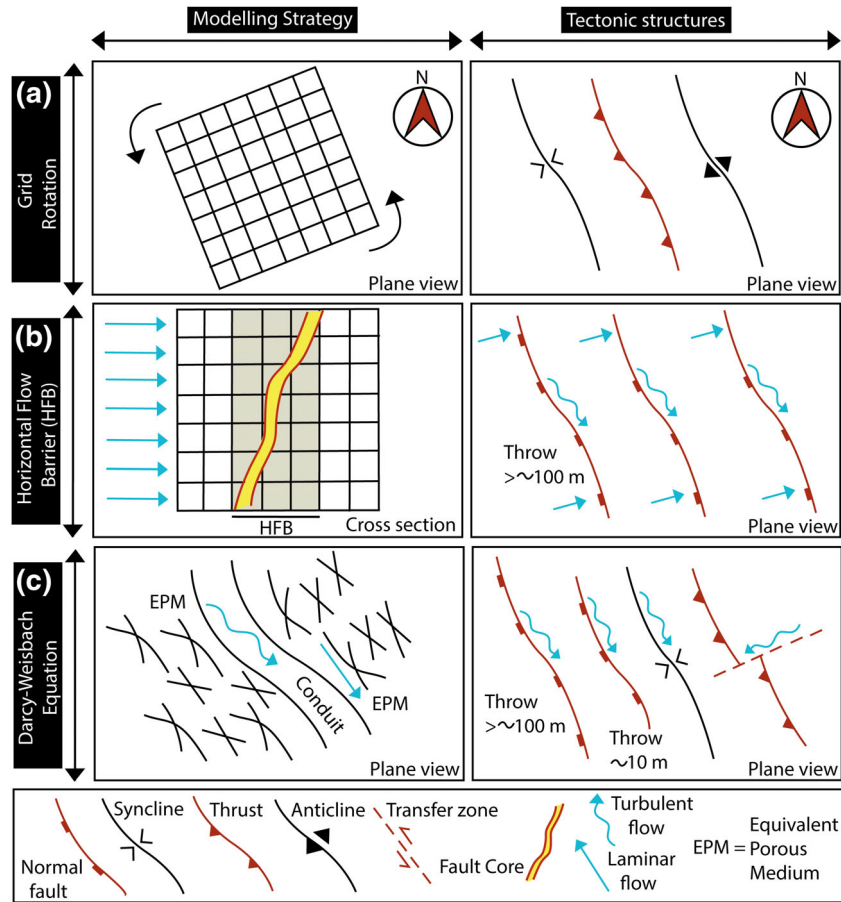
Figure 9. Groundwater flow in fractured carbonate aquifers; modeling strategy versus tectonic structure using the EPM and CN approaches: (a) grid rotation for, (b) Horizontal Flow Barrier for EPM, (c) Darcy-Weisbach equation for CN inserted into an EPM.

hydraulic head loss along the pipe. A number of authors have applied Equations 1 and 2 to MODFLOW-2005, who found the models are highly sensitive to the diameter (d) of conduits (Shoemaker et al. 2008; Hill et al. 2010; Gallegos et al. 2013; Saller et al. 2013; Medici et al. 2019b).

In summary, Equations 1 and 2 describe laminar and turbulent flow, respectively, in pipe conduits of a certain diameter and surface roughness. Conduits elongated parallel to the syncline axes have been described by speleologists and geomorphologists as pipes of diameters in the range approximately 0.5 – 5 m (Murphy 2000; Ford and Williams 2013). Springs have been found in karst environments connected to pipe-shaped caves in the Alps in France, Switzerland, Austria, and Germany, in the Appennines in Italy and in the Woodville karst plain in Florida (Figure 2a; Király 1975; Falcone et al. 2008, 2012; Shoemaker et al. 2008; Goldscheider and Drew 2014). The Darcy-Weisbach equations have been incorporated by the United States Geological Survey (USGS) in the Conduit Flow Process Mode-1 (CFPM-1) Package of MODFLOW-2005 to model flow in such pipe-shape conduits and represent carbonate aquifers as dual porosity media (Shoemaker et al. 2008; Hill et al. 2010).

The CFPM-1 modeling solution is used to account for the preferential-flow pathway behavior of normal faults at a range of scales in carbonate aquifers (Figure 9c; Hsieh and Freckleton 1993; Caine et al. 1996; Shoemaker et al. 2008; Faulkner et al. 2010; Hill et al. 2010; Bense et al. 2013). More in detail, flow through pipes, which is described by Equations 1 and 2, is inserted in specific fault segments, which are characterized by alignment of springs, dolines and caves. However, this modeling solution must be coupled with the HFB Package to also account for the barrier behavior of large (throw > ∼100 m) scale normal faults.

The HFB Package is inserted in portions of the model domain that are characterized by sharp drops of the piezometric surface moving from the hanging wall to the footwall blocks to account for the across-strike barrier behavior of normal faults (Hsieh and Freckleton 1993; Mohamed and Worden 2006; Chaussard et al. 2014; Hanson et al. 2014). A valid and alternative method proposed by the USGS to model turbulent flow is the Conduit Flow Process Mode-2 (CFPM-2). This solution consists of representing turbulence in a network of large pores with a specific average diameter (Shoemaker et al. 2008; Reimann and Hill 2009; Reimann et al. 2011; Xu et al. 2015). In the latter method that is mathematically

described in detail in Reimann et al. (2011), the flow velocity under laminar and turbulent flow conditions is described by the Equation 3.

$$V = \frac{Re}{dk} \qquad (3)$$

where Re is the Reynolds number, d (L) is the mean void diameter, and k (L^2/T) is the kinematic viscosity of water. Users only need to assign upper and lower Re, the mean groundwater temperature for computing viscosity, and mean void diameters. Hence, this numerical methodology does not require a detailed geometrical definition of the CNs and can be coupled with the CFPM-1 accounting for turbulence both in discrete conduits and in the interbedded matrix. Consequently, CFPM-2 has been used to describe turbulent flow in fractured limestones in a number of numerical models. Despite this, we retain, in agreement with the developers of the conduit flow process (see Shoemaker et al. 2008), that this strategy is more appropriate to represent turbulence in carbonate rocks with paleobiogenic origin such as tufa and travertine. In these kind of carbonate rocks, a network of large and connected pores of sedimentary origin is effectively present (Love and Chafetz 1988; Guo and Riding 1994). The CFPM-2 is inserted in specific layers that are characterized by large pores, where turbulent flow occurs. Other layers that correspond to parts of the stratigraphic succession with smaller voids are instead modeled using laminar/Darcian flow in the EPM (Shoemaker et al. 2008; Reimann et al. 2011). In the case of travertine or tufa and the occurrence of a valley where intense groundwater flow and karst conduits occur; the CFPM-1 and CFPM-2 approaches can be combined in the 3D domain to model turbulence in pipe-shaped conduits and large pores of sedimentary origin, respectively (Shoemaker et al. 2008).

Discrete Fracture Network

DFN modeling generates distributions of fractures and bedding planes and compares these discontinuities with observed data from outcrop scanline and/or borehole acoustic televiewer logging to represent their position, size, and mechanical aperture (Parker et al. 2019). These DFN models can be generated either from a combination of outcrop mapping, borehole data, and seismic data (e.g., Kattenhorn and Pollard 2001; Cvetkovic et al. 2004; Panza et al. 2015; Zambrano et al. 2016; Giuffrida et al. 2020), or from using a stochastic approach in case of limited data availability (e.g., Voeckler and Allen 2012; Hyman et al. 2015; Lei et al. 2017; Lepillier et al. 2020). Mechanical stratigraphy plays an important role in the fracture network geometry as well as in the resultant groundwater flow (e.g., Cooke et al. 2006). Therefore, capturing the heterogeneities and variations in mechanical layering is of paramount importance when generating DFN models. Combination of suitable algorithms and availability of data will lead to a more realistic modeled fracture distribution in carbonate aquifers. In fact, the fracture data from outcrops, alone, cannot adequately

represent the complexity of geological structures in the subsurface. Lemieux et al. (2006) combined outcrop and core data to generate a realistic DFN model at a small scale ($\sim$10^0 m in lengths) in a dolostone of Silurian age in Ontario. However, the use of seismic data can lead to a larger scale ($\sim$10^1 m in lengths) and a deeper ($\sim$10^2–10^3 meters below the ground level) representation of the DFN, as the 3D fracturing network can also be geophysically generated by combining fracture data from acoustic televiewer logging with seismic attributes. In this approach, the scale gap between the dataset from wells is bridged by the use of seismic data in sedimentary rocks (Botter et al. 2017a, 2017b). Recently, seismic data of the Cretaceous carbonates in the Danish North Sea has been utilized to characterize the fracture network for flow modeling applications (Aabø et al. 2020).

In contrary to EPM approach, DFN models are supported by unstructured grids and do not require rotating grids to represent the flow properties in the presence of a dominant set of sub-vertical joints. The generated fracture sets are then added into a flow model (e.g., MAFIC, ConnectiveFlow, dfnWorks, DFNFlow, HGS, CRAK, and SMOKER) to derive estimates of the bedrock hydraulic conductivity (Neuman 2005; Rutqvist et al. 2013; Hyman et al. 2015). Rock discontinuities are assumed permeable as supported by well-testing data and must be assigned a hydraulic aperture to provide a fracture transmissivity in the carbonate rock mass (Selroos et al. 2002; Parker et al. 2019). The use of seismic data to map the fracture hydraulic properties at depth (e.g., effective fracture porosity and hydraulic conductivity) can also lower uncertainties associated with the properties of rocks located away from the wells (e.g., Parra et al. 2006; Parra and Emery 2013). Recent advances in DFN groundwater flow and transport modeling couple advective flow through the fractures with diffusivity in the matrix blocks (Parker et al. 2019). In their workflow, Parker et al. (2019) couple DFN and EPM approaches using the FRACTRAN numerical code leading to match model outputs with information from wells on the dispersal of monitored plumes at industrial field sites. The latter approach contrasts a number of researches (e.g., Benke and Painter 2003; Voeckler and Allen 2012; Hyman et al. 2015) that neglect diffusion in the matrix that increases the computational efforts.

Discussion

We presented the strategies for modeling groundwater flow in the presence of different tectonic structures with regards to the three approaches, EPM, CFPM-1, 2, and DFN, used to model groundwater flow and contaminant transport in carbonate aquifers (Figure 8; Selroos et al. 2002; Shoemaker et al. 2008). The choice of modeling approach primarily depends on interplays between the observation scale, degree of karstification, hydraulic behavior (barrier vs. conduit), and orientation of the rock discontinuities. The easiest numerical solution in terms of computational efforts is represented by the

exclusive Darcian flow in an EPM (Chapman et al. 2013). This choice is considered reasonable when observations at the outcrop scale match structural maps in terms of orientation of the rock discontinuities (Odling et al. 1999; Lemieux et al. 2006). In the latter case of consistent orientation of fractures from outcrop up to groundwater flow model scale, one horizontal grid axis can be oriented parallel to the Fisher mean vector of high angle fold-related fractures measured in outcrops. However, a combination of two or three approaches is needed to model fluid flow in a variety of case studies to represent the complexity of carbonate aquifers.

Groundwater flow models at the scale of multiple industrial plants (∼0.5–10 km) and single watersheds (∼0.1–100 km) use conduits embedded within an EPM approach at relatively shallow (<∼0.1 km) depths (Figure 9c; Gallegos et al. 2013; Chen and Goldscheider 2014; Saller et al. 2013; Medici et al. 2019b). However, groundwater flow models only account for a CN approach in some case studies in fold and thrust belts. In such cases, elevated hydraulic gradients are responsible for a high degree of karstification and flow is largely dominated by cavities that are a few meters wide. Turbulent flow occurs in carbonate aquifers under such hydrogeological conditions (Hill et al. 2010).

DFN models are used to represent groundwater flow at the scale of the industrial field site to predict the dispersal of plumes in approximately 0.3–5 km length in less intensively karstified carbonate aquifers (Chapman and Parker 2005; Parker et al. 2008; Cheong et al. 2017). The availability of wells in a relatively small area coupled with 1D scanline measurements allows the network of bedding plane discontinuities and fractures to be defined in three dimensions at high resolution. At the scale of an industrial site (∼0.3–5 km), recent applications in the fractured Silurian Dolostone of Ontario allow the coupling of a DFN with an EPM approach to simulate advective and diffusive flow in fractures and the matrix, respectively (Parker et al. 2019). Here, karstic features were not detected by acoustic and televiewer logging due to the choice of neglecting the CN approach. The combination of a DFN with an EPM approach applied to the Silurian Dolostone of Ontario is called DFN-M. This approach has been successful in matching experimental data on the spatial distribution of a monitored groundwater plume with a contaminant transport model.

However, a future research scenario could involve combining the CN with a DFN approach to model fluid flow in lithoid carbonate aquifers. Indeed, cavities of diameters of a few centimeters are present in carbonate aquifers even in areas characterized by relatively low hydraulic gradients, flat topography, and sub-horizontal beds where the stratigraphic succession is faulted (Murphy 2000; Medici et al. 2019b). The coupling of a DFN with a CN approach can also have an impact on modeling flow at much higher depths (∼1–3 km) in medium- and high-enthalpy geothermal reservoirs. Paleokarst features in bedding plane discontinuities and sub-vertical joints were detected at these greater depths significantly

influencing the recovery of production wells (Bauer and Tóth 2017). A DFN must be coupled to a CN to represent fluid flow in marine carbonate rocks that have been exposed to episodes of emersion and erosion, and hence to the development of paleokarst cavities (Vecsei and Sanders 1997; Brandano 2017). The combination of a DFN and a CN approach can be beneficial to either the chemical industry for managing the contaminant plume or the geothermal energy sector.

However, maximum complexity in terms of computation efforts may be necessary to model fluid flow in deep aquifers exploited to recover hot water mixed with vapor in porous carbonates. In this case, the EPM approach must be used, and the 3D domain should be divided by hydrofacies to account for the significant flow component occurring within the matrix. Residual fracture and channel flow in paleokarst conduits occurs under pumping conditions and hence the discrete fracture and CNs need to be inserted to the 3D models (Bauer and Tóth 2017; Medici et al. 2018; Tomassetti et al. 2018).

Conclusions

Groundwater flow is challenging to model in carbonate aquifers due to interplays between brittle tectonic structures and karstification. Fluid flow is controlled by rock discontinuities, which are represented by bedding plane and tectonic fractures in shallow carbonate aquifers across the world. Consequently, modeling strategies must be reviewed in relation to the pattern of rock discontinuity as well as the degree of karstification using the three different existing approaches (EPM, CN, and DFN) developed to model groundwater flow in porous and fractured rocks. The findings of our review can be summarized in four key points:

1. Rotating the grids using an EPM approach is recommended for mountain belt settings to account for higher hydraulic conductivity parallel to the fold axis from the scale of a few up to tens of kilometers. The same strategy is appropriate to model fluid flow in unfaulted areas using an EPM approach in jointed and highly horizontally anisotropic carbonate aquifers. In these geological media, sub-vertical joints are characterized by a dominant set according to discontinuity surveys undertaken in quarries and cliffs across Europe and northern America.
2. Rapid groundwater flow and karstification occurs in synclines, normal faults, and thrusts in limestone and dolostone aquifers. Systems of caves and cavities occur and groundwater flow models need to be locally modified to represent turbulence. Hence, a CN approach is needed to insert channels characterized by turbulent flow embedded in an EPM.
3. The DFN approach is supported by unstructured grids enabling 3D representation of fractures contributing to fluid flow. This approach is used at the scale of the 0.3–5 km in less heavily karstified aquifers and has been recently combined with an EPM approach to

simulate contaminant transport in the low conductive matrix.

4. Combining an EPM method with DFN and CN methods represents a future research approach that is not currently practiced in hydrogeology. The EPM method is needed in porous carbonate rocks in deep aquifers due to the significant component of matrix flow. However, discrete fractures and conduits still influence flow to pumped wells in medium and high enthalpy geothermal reservoirs and need therefore to be inserted in the 3D domain.

Overall, networks of fractures and karst conduits highly control groundwater flow in carbonate aquifers and major groundwater resources are here stored. Hence, specific guidelines are needed in faulted and unfaulted areas to better represent fluid flow in these geological media combining the three existing methodologies: EPM, CN, and DFN.

Acknowledgments

References

Aabø, T.M., J.S. Dramsch, C.L. Würtzen, S. Seyum, and M. Welch. 2020. An integrated workflow for fracture characterization in chalk reservoirs, applied to the Kraka Field. *Marine and Petroleum Geology* 112: 104065.

Agosta, F., M. Alessandroni, M. Antonellini, E. Tondi, and M. Giorgioni. 2010. From fractures to flow: A field-based quantitative analysis of an outcropping carbonate reservoir. *Tectonophysics* 490: 197–213.

Agosta, F., and A. Aydin. 2006. Architecture and deformation mechanism of a basin-bounding normal fault in Mesozoic platform carbonates, central Italy. *Journal of Structural Geology* 28, no. 8: 1445–1467.

Agosta, F., and D.L. Kirschner. 2003. Fluid conduits in carbonate-hosted seismogenic normal faults of central Italy.

Journal of Geophysical Research: Solid Earth 108, no. B4. https://doi.org/10.1029/2002JB002013

Al-Hinai, S., Q.J. Fisher, B. Al-Busafi, P. Guise, and C.A. Grattoni. 2008. Laboratory measurements of the relative permeability of cataclastic fault rocks: An important consideration for production simulation modelling. *Marine and Petroleum Geology* 25, no. 6: 473–485.

Aldrick, R.J. 1978. The hydrogeology of the magnesian limestones in Yorkshire between the River Wharfe and the River Aire. *Quarterly Journal of Engineering Geology and Hydrogeology* 11, no. 2: 193–201.

Allen, D.J., L.M. Brewerton, B.R. Colebee, M.A. Gibbs, A. Lewis, S.J. MacDonald, A.T. Wagstaff, and L.J. Williams. 1997. *The Physical Properties of Major Aquifers in England and Wales*. Technical Report WD/97/34, 157-287. Nottingham, UK: British Geological Survey.

Allmendinger, R.W. 1998. Inverse and forward numerical modeling of trishear fault-propagation folds. *Tectonics* 17, no. 4: 640–656.

Amraoui, F., M. Razack, and L. Bouchaou. 2003. Turbidity dynamics in karstic systems. Example of Ribaa and Bittit springs in the Middle Atlas (Morocco). *Hydrological Sciences Journal* 48, no. 6: 971–984.

Amoruso, A., L. Crescentini, M. Petitta, and M. Tallini. 2013. Parsimonious recharge/discharge modeling in carbonate fractured aquifers: The groundwater flow in the Gran Sasso aquifer (central Italy). *Journal of Hydrology* 476: 136–146.

Angelini, P., and W. Dragoni. 1997. The problem of modeling limestone springs: The case of Bagnara (North Apennines, Italy). *Groundwater* 35, no. 4: 612–618.

Antonellini, M., L. Petracchini, A. Billi, and D. Scrocca. 2014. First reported occurrence of deformation bands in a platform limestone, the Jurassic Calcare Massiccio Fm., northern Apennines, Italy. *Tectonophysics* 628: 85–104.

Antonellini, M., E. Tondi, F. Agosta, A. Aydin, and G. Cello. 2008. Failure modes in deep-water carbonates and their impact for fault development: Majella Mountain, Central Apennines, Italy. *Marine and Petroleum Geology* 25, no. 10: 1074–1096.

Assari, A., and Z. Mohammadi. 2017. Assessing flow paths in a karst aquifer based on multiple dye tracing tests using stochastic simulation and the MODFLOW-CFP code. *Hydrogeology Journal* 25, no. 6: 1679–1702.

Aydin, A. 2000. Fractures, faults, and hydrocarbon entrapment, migration and flow. *Marine and Petroleum Geology* 17, no. 7: 797–814.

Bakalowicz, M. 2015. Karst and karst groundwater resources in the Mediterranean. *Environmental Earth Sciences* 74, no. 1: 5–14.

Bales, R.C., C.P. Gerba, G.H. Grondin, and J.L. Jensen. 1989. Bacteriophage transport in sandy soil and fractured tuff. *Applied and Environmental Microbiology* 55, no. 8: 2061–2067.

Barrash, W., and M.E. Dougherty. 1997. Modeling axially symmetric and nonsymmetric flow to a well with MODFLOW, and application to Goddard2 well test, Boise, Idaho. *Groundwater* 35, no. 4: 602–611.

Bauer, M., and T.M. Tóth. 2017. Characterization and DFN modelling of the fracture network in a Mesozoic karst reservoir: Gomba oilfield, Paleogene Basin, Central Hungary. *Journal of Petroleum Geology* 40, no. 3: 319–334.

Bauer, H., T.C. Schröckenfuchs, and K. Decker. 2016. Hydrogeological properties of fault zones in a karstified carbonate aquifer (Northern Calcareous Alps, Austria). *Hydrogeology Journal* 24: 1147–1170.

Bauer, S., R. Liedl, and M. Sauter. 2003. Modeling of karst aquifer genesis: Influence of exchange flow. *Water Resources Research* 39, no. 10. https://agupubs.onlinelibrary.wiley.com/doi/full/10.1029/2003WR002218

Benke, R., and S. Painter. 2003. Modeling conservative tracer transport in fracture networks with a hybrid approach based

on the Boltzmann transport equation. *Water Resources Research* 39, no. 11. https://agupubs.onlinelibrary.wiley.com/doi/full/10.1029/2003WR001966

Bense, V.F., T. Gleeson, S.E. Loveless, O. Bour, and J. Scibek. 2013. Fault zone hydrogeology. *Earth-Science Reviews* 127: 171–192.

Berkowitz, B. 2002. Characterizing flow and transport in fractured geological media: A review. *Advances in Water Resources* 25: 861–884.

Bidaux, P., and C. Drogue. 1993. Calculation of low-range flow velocities in fractured carbonate media from borehole hydrochemical logging data comparison with thermometric results. *Groundwater* 31: 19–26.

Billi, A., A. Valle, M. Brilli, C. Faccenna, and R. Funiciello. 2007. Fracture-controlled fluid circulation and dissolutional weathering in sinkhole-prone carbonate rocks from central Italy. *Journal of Structural Geology* 29, no. 3: 385–395.

Billi, A. 2005. Attributes and influence on fluid flow of fractures in foreland carbonates of southern Italy. *Journal of Structural Geology* 27: 1630–1643.

Billi, A., F. Salvini, and F. Storti. 2003. The damage zone-fault core transition in carbonate rocks: Implications for fault growth, structure and permeability. *Journal of Structural Geology* 25, no. 11: 1779–1794.

Boni, C., P. Bono, and G. Capelli. 1986. Schema idrogeological dell'Italia centrale. *Memorie della Societa Geologica Italiana* 35: 991–1012.

Borović, S., J. Terzić, and M. Pola. 2019. Groundwater quality on the adriatic karst Island of Mljet (Croatia) and its implications on water supply. *Geofluids* 20: 1–14. https://doi.org/10.1155/2019/5142712

Boyer, S.E., and D. Elliot. 1982. Thrust systems. *AAPG Bulletin* 66, no. 9: 1196–1230.

Botter, C., N. Cardozo, I. Lecomte, A. Rotevatn, and G. Paton. 2017a. The impact of faults and fluid flow on seismic images of a relay ramp over production time. *Petroleum Geoscience* 23: 17–28.

Botter, C., N. Cardozo, D. Qu, J. Tveranger, and D. Kolyukhin. 2017b. Seismic characterization of fault facies models. *Interpretation* 5: SP9–SP26.

Brandano, M. 2017. Unravelling the origin of a Paleogene unconformity in the Latium-Abruzzi carbonate succession: A shaved platform. *Palaeogeography, Palaeoclimatology, Palaeoecology* 485: 687–696.

Bucci, A., E. Petrella, G. Naclerio, S. Gambatese, and F. Celico. 2014. Bacterial migration through low-permeability fault zones in compartmentalised aquifer systems: A case study in southern Italy. *International Journal of Speleology* 43, no. 3: 273–281.

Caine, J.S., J.P. Evans, and C.B. Forster. 1996. Fault zone architecture and permeability structure. *Geology* 24, no. 11: 1025–1028.

Carminati, E., D. Scrocca, and C. Doglioni. 2010. Compaction-induced stress variations with depth in an active anticline: Northern Apennines, Italy. *Journal of Geophysical Research: Solid Earth* 115, no. B2. https://doi.org/10.1029/2009JB006395

Carminati, E., M. Cuffaro, and C. Doglioni. 2009. Cenozoic uplift of Europe. *Tectonics* 28, no. 4. https://doi.org/10.1029/2009TC002472

Celico, F., E. Petrella, and P. Celico. 2006. Hydrogeological behaviour of some fault zones in a carbonate aquifer of southern Italy: An experimentally based model. *Terra Nova* 18, no. 5: 308–313.

Chapman, S.W., B.L. Parker, J.A. Cherry, S.D. McDonald, K.J. Goldstein, J.J. Frederick, D.J.S. Germain, D.M. Cutt, and C.E. Williams. 2013. Combined MODFLOW-FRACTRAN application to assess chlorinated solvent transport and remediation in fractured sedimentary rock. *Remediation Journal* 23, no. 3: 7–35.

Chapman, S.W., and B.L. Parker. 2005. Plume persistence due to aquitard back diffusion following dense non-aqueous phase liquid source removal or isolation. *Water Resources Research* 41, no. 12. https://doi.org/10.1029/2005WR004224

Chaussard, E., R. Bürgmann, M. Shirzaei, E.J. Fielding, and B.L. Baker. 2014. Predictability of hydraulic head changes and characterization of aquifer-system and fault properties from InSAR-derived ground deformation. *Journal of Geophysical Research: Solid Earth* 119, no. 8: 6572–6590.

Cheong, J.Y., S.Y. Hamm, D.H. Lim, and S.G. Kim. 2017. Hydraulic parameter generation technique using a discrete fracture network with bedrock heterogeneity in Korea. *Water* 9, no. 12. https://doi.org/10.3390/w9120937

Chen, Z., and N. Goldscheider. 2014. Modeling spatially and temporally varied hydraulic behavior of a folded karst system with dominant conduit drainage at catchment scale, Hochifen–Gottesacker, Alps. *Journal of Hydrology* 514: 41–52.

Cilona, A., P. Baud, E. Tondi, F. Agosta, S. Vinciguerra, A. Rustichelli, and C.J. Spiers. 2012. Deformation bands in porous carbonate grainstones: Field and laboratory observations. *Journal of Structural Geology* 45: 137–157.

Cooke, M.L., J.A. Simo, C.A. Underwood, and P. Rijken. 2006. Mechanical stratigraphic controls on fracture patterns within carbonates and implications for groundwater flow. *Sedimentary Geology* 184: 225–239.

Cosentino, D., P. Cipollari, P. Marsili, and D. Scrocca. 2010. Geology of the central Apennines: A regional review. *Journal of the Virtual Explorer* 36, no. 11: 1–37.

Cvetkovic, V., S. Painter, N. Outters, and J.O. Selroos. 2004. Stochastic simulation of radionuclide migration in discretely fractured rock near the Äspö Hard Rock Laboratory. *Water Resources Research* 40, no. 2. https://doi.org/10.1029/2003WR002655

Dausse, A., V. Leonardi, and H. Jourde. 2019. Hydraulic characterization and identification of flow-bearing structures based on multi-scale investigations applied to the Lez karst aquifer. *Journal of Hydrology Regional Studies* 26: 100627.

Dawers, N.H., and M.H. Anders. 1995. Displacement-length scaling and fault linkage. *Journal of Structural Geology* 17, no. 5: 607–614.

Douglas, A.A., L.J. Osiensky, and C.K. Keller. 2007. Carbon-14 dating of ground water in the Palouse Basin of the Columbia River basalts. *Journal of Hydrology* 334: 502–512.

Ely, D.M., E.R. Burns, D.S. Morgan, J.J. Vaccaro. 2014. Numerical simulation of groundwater flow in the Columbia Plateau Regional Aquifer System, Idaho, Oregon, and Washington. U.S. Geological Survey Report 5127, 90.

Ely, D.M., M.P. Bachmann, and J.J. Vaccaro. 2011. *Numerical Simulation of Groundwater Flow for the Yakima River Basin Aquifer System*. Washington, DC: U.S. Geological Survey.

Evans, M.A., and M.P. Fischer. 2012. On the distribution of fluids in folds: A review of controlling factors and processes. *Journal of Structural Geology* 44: 2–24.

Falcone, A.R., V. Carucci, A. Falgiani, M. Manetta, B. Parisse, M. Petitta, S. Rusi, M. Spizzico, and M. Tallini. 2012. Changes on groundwater flow and hydrochemistry of the Gran Sasso carbonate aquifer after 2009 l'Aquila earthquake. *International Journal of Geosciences* 131, no. 3: 450–474.

Falcone, R.A., A. Falgiani, B. Parisse, M. Petitta, M. Spizzico, and M. Tallini. 2008. Chemical and isotopic ($\delta18O‰$, $\delta2H‰$, $\delta13C‰$, 222Rn) multi-tracing for groundwater conceptual model of carbonate aquifer (Gran Sasso INFN underground laboratory—central Italy). *Journal of Hydrology* 357: 368–388.

Farrant, A.R., and A.H. Cooper. 2008. Karst geohazards in the UK: The use of digital data for hazard management. *Quarterly Journal of Engineering Geology and Hydrogeology* 41, no. 3: 339–356.

Faulkner, D.R., C.A.L. Jackson, R.J. Lunn, R.W. Schlische, Z.K. Shipton, C.A.J. Wibberley, and M.O. Withjack. 2010. A review of recent developments concerning the structure, mechanics and fluid flow properties of fault zones. *Journal of Structural Geology* 32, no. 11: 1557–1575.

Fiorillo, F., M. Petitta, E. Preziosi, S. Rusi, L. Esposito, and M. Tallini. 2015. Long-term trend and fluctuations of karst spring discharge in a Mediterranean area (central-southern Italy). *Environmental Earth Sciences* 74: 153–172.

Fisher, Q.J., J. Haneef, C.A. Grattoni, S. Allshorn, and P. Lorinczi. 2018. Permeability of fault rocks in siliciclastic reservoirs: Recent advances. *Marine and Petroleum Geology* 91: 29–42.

Fisher, Q.J., and R.J. Knipe. 2001. The permeability of faults within siliciclastic petroleum reservoirs of the North Sea and Norwegian Continental Shelf. *Marine and Petroleum Geology* 18, no. 10: 1063–1081.

Flügel, E. 2013. *Microfacies of Carbonate Rocks: Analysis, Interpretation and Application*. Berlin, Germany: Springer Science & Business Media.

Ford, D., and P.D. Williams. 2013. *Karst Hydrogeology and Geomorphology*. New York: John Wiley & Sons.

Gallegos, J.J., B.X. Hu, and H. Davis. 2013. Simulating flow in karst aquifers at laboratory and sub-regional scales using MODFLOW-CFP. *Hydrogeology Journal* 21, no. 8: 1749–1760.

Ghasemizadeh, R., F. Hellweger, C. Butscher, I. Padilla, D. Vesper, M. Field, and A. Alshawabkeh. 2012. Review: Groundwater flow and transport modeling of karst aquifers, with particular reference to the North Coast Limestone aquifer system of Puerto Rico. *Hydrogeology Journal* 20, no. 8: 1441–1461.

Giacopetti, M., M. Materazzi, G. Pambianchi, and K. Posavec. 2017. Analysis of mountain springs discharge time series in the Tennacola stream catchment (Central Apennine, Italy). *Environmental Earth Sciences* 76, no. 1: 20–31.

Gillespie, P.A., J.J. Walsh, J. Watterson, C.G. Bonson, and T. Manzocchi. 2001. Scaling relationships of joint and vein arrays from The Burren, Co. Clare, Ireland. *Journal of Structural Geology* 23: 183–201.

Giuffrida, A., F. Agosta, A. Rustichelli, E. Panza, V. La Bruna, M. Eriksson, S. Torrieri, and M. Giorgioni. 2020. Fracture stratigraphy and DFN modelling of tight carbonates, the case study of the lower cretaceous carbonates exposed at the Monte Alpi (Basilicata, Italy). *Marine and Petroleum Geology* 112: 104045.

Goldscheider, N. 2012. A holistic approach to groundwater protection and ecosystem services in karst terrains. *AQUA Mundi* 3, no. 2: 117–124.

Goldscheider, N., and D. Drew. 2014. *Methods in Karst Hydrogeology: IAH: International Contributions to Hydrogeology*. Boca Raton, Florida: CRC Press.

Goldscheider, N., J. Mádl-Szőnyi, A. Erőss, and E. Schill. 2010. Review: Thermal water resources in carbonate rock aquifers. *Hydrogeology Journal* 18, no. 6: 1303–1318.

Goldscheider, N. 2005. Fold structure and underground drainage pattern in the alpine karst system Hochifen-Gottesacker. *Eclogae Geologicae Helvetiae* 98: 1–17.

Göppert, N., N. Goldscheider, and H. Scholz. 2011. Karst geomorphology of carbonatic conglomerates in the folded Molasse zone of the Northern Alps (Austria/Germany). *Geomorphology* 130: 289–298.

Göppert, N., and N. Goldscheider. 2008. Solute and colloid transport in karst conduits under low-and high-flow conditions. *Groundwater* 46: 61–68.

Gremaud, V., N. Goldscheider, L. Savoy, G. Favre, and H. Masson. 2009. Geological structure, recharge processes and underground drainage of a glacierised karst aquifer system, Tsanfleuron-Sanetsch, Swiss Alps. *Hydrogeology Journal* 17, no. 8: 1833–1848.

Guo, Z., G.E. Fogg, M.L. Brusseau, E.M. LaBolle, and J. Lopez. 2019. Modeling groundwater contaminant transport in the presence of large heterogeneity: A case study comparing MT3D and RWhet. *Hydrogeology Journal* 27, no. 4: 1363–1371.

Guo, F., G. Jiang, D. Yuan, and J.S. Polk. 2013. Evolution of major environmental geological problems in karst areas of southwestern China. *Environmental Earth Sciences* 69, no. 7: 2427–2435.

Guo, L., and R. Riding. 1994. Origin and diagenesis of quaternary travertine shrub fabrics, Rapolano Terme, Central Italy. *Sedimentology* 41, no. 3: 499–520.

Hanson, R.T., E.F. Lorraine, C. Claudia, C. Faunt, D.R. Gibbs, and W. Schmid. 2014. Hydrologic models and analysis of water availability in Cuyama Valley, California. No. 2014-5150. U.S. Geological Survey, Scientific Investigations Report 2014-5150.

Harbaugh A.W. 2005. MODFLOW-2005, the U.S. Geological Survey modular ground-water model—The ground-water flow process. U.S. Geological Survey, Techiniques and Methods Report 6-A16.

Hartmann, A., and A. Baker. 2017. Modeling karst vadose zone hydrology and its relevance for palaeoclimate reconstruction. *Earth Science Reviews* 172: 178–192.

Hartmann, A., N. Goldscheider, T. Wagener, J. Lange, and M. Weiler. 2014a. Karst water resources in a changing world: Review of hydrological modeling approaches. *Reviews of Geophysics* 52, no. 3: 218–242.

Hartmann, A., M. Mudarra, B. Andreo, A. Marín, T. Wagener, and J. Lange. 2014b. Modeling spatiotemporal impacts of hydroclimatic extremes on groundwater recharge at a Mediterranean karst aquifer. *Water Resources Research* 50, no. 8: 6507–6521.

Hartmann, S., N.E. Odling, and L.J. West. 2007. A multidirectional tracer test in the fractured chalk aquifer of E. Yorkshire, UK. *Journal of Contaminant Hydrology* 94: 315–331.

Hill, M.E., M.T. Stewart, and A. Martin. 2010. Evaluation of the MODFLOW-2005 conduit flow process. *Groundwater* 48, no. 4: 549–559.

Hyman, J.D., S. Karra, N. Makedonska, C.W. Gable, S.L. Painter, and H.S. Viswanathan. 2015. dfnWorks: A discrete fracture network framework for modeling subsurface flow and transport. *Computational Geosciences* 84: 10–19.

Hsieh, P.A., and J.R. Freckleton. 1993. Documentation of a computer program to simulate horizontal-flow barriers using the U.S. Geological Survey's modular three-dimensional finite-difference ground-water flow model. U.S. Geological Survey, Open-File Report 92-477.

Jolivet, L., and C. Faccenna. 2000. Mediterranean extension and the Africa-Eurasia collision. *Tectonics* 19, no. 6: 1095–1106.

Jourde, H., P. Fenart, M. Vinches, S. Pistre, and B. Vayssade. 2007. Relationship between the geometrical and structural properties of layered fractured rocks and their effective permeability tensor. A simulation study. *Journal of Hydrology* 337: 117–132.

Jourde, H., S. Pistre, P. Perrochet, and C. Drogue. 2002. Origin of fractional flow dimension to a partially penetrating well in stratified fractured reservoirs. New results based on the study of synthetic fracture networks. *Advances in Water Resources* 25, no. 4: 371–387.

Kalhor, K., R. Ghasemizadeh, L. Rajic, and A. Alshawabkeh. 2019. Assessment of groundwater quality and remediation in karst aquifers: A review. *Groundwater for Sustainable Development* 8: 104–121.

Kaminskaite, I., Q.J. Fisher, and E.A.H. Michie. 2019. Microstructure and petrophysical properties of deformation bands in high porosity carbonates. *Journal of Structural Geology* 119: 61–80.

Kattenhorn, S.A., and D.D. Pollard. 2001. Integrating 3-D seismic data, field analogs, and mechanical models in the analysis of segmented normal faults in the Wytch farm oil field, southern England, United Kingdom. *AAPG Bulletin* 85, no. 7: 1183–1210.

Király, L. 1975. Rapport sur l'état actuel des connaissances dans le domaine des caractères physiques des roches karstiques. International Union of Geological. *Sciences* 3: 53–67.

Korneva, I., E. Tondi, F. Agosta, A. Rustichelli, V. Spina, R. Bitonte, and R. Di Cuia. 2014. Structural properties of fractured and faulted Cretaceous platform carbonates, Murge Plateau (southern Italy). *Marine and Petroleum Geology* 57: 312–326.

Kresic, N. 1995. Remote sensing of tectonic fabric controlling groundwater flow in Dinaric Karst. *Remote Sensing of Environment* 53, no. 2: 85–90.

Lacombe, P.J., and W.C. Burton. 2010. Hydrogeologic framework of fractured sedimentary rock, Newark Basin, New Jersey. *Groundwater Monitoring & Remediation* 30, no. 2: 35–45.

Lauber, U., and N. Goldscheider. 2014. Use of artificial and natural tracers to assess groundwater transit-time distribution and flow systems in a high-alpine karst system (Wetterstein Mountains, Germany). *Hydrogeology Journal* 22, no. 8: 1807–1824.

Lei, Q., J.P. Latham, and C.F. Tsang. 2017. The use of discrete fracture networks for modelling coupled geomechanical and hydrological behaviour of fractured rocks. *Computational Geotechnics* 85: 151–176.

Lemieux, J.M., R. Therrien, and D. Kirkwood. 2006. Small scale study of groundwater flow in a fractured carbonate-rock aquifer at the St-Eustache quarry, Québec, Canada. *Hydrogeology Journal* 14, no. 4: 603–612.

Lepillier, B., P.O. Bruna, D. Bruhn, E. Bastesen, A. Daniilidis, Ó. Garcia, A. Torabi, and W. Wheeler. 2020. From outcrop scanlines to discrete fracture networks, an integrative workflow. *Journal of Structural Geology*: 133. https://doi.org/10.1016/j.jsg.2020.103992

Love, K.M., and H.S. Chafetz. 1988. Diagenesis of laminated travertine crusts, Arbuckle Mountains, Oklahoma. *Journal of Sedimentary Research* 58, no. 3: 441–445.

Mahler, B.J., and B.D. Garner. 2009. Using nitrate to quantify quick flow in a karst aquifer. *Groundwater* 47, no. 3: 350–360.

Maloszewski, P., W. Stichler, A. Zuber, and D. Rank. 2002. Identifying the flow systems in a karstic-fissured-porous aquifer, the Schneealpe, Austria, by modelling of environmental 18O and 3H isotopes. *Journal of Hydrology* 256: 48–59.

Masciopinto, C., and D. Palmiotta. 2013. Relevance of solutions to the Navier-Stokes equations for explaining groundwater flow in fractured karst aquifers. *Water Resources Research* 49, no. 6: 3148–3164.

Maurice, L.D., T.C. Atkinson, J.A. Barker, J.P. Bloomfield, A.R. Farrant, and A.T. Williams. 2006. Karstic behaviour of groundwater in the English chalk. *Journal of Hydrology* 330: 63–70.

Medici, G., P. Bajak, L.J. West, P.J. Chapman, and S.A. Banwart. 2020. DOC and nitrate fluxes from farmland; impact on a dolostone aquifer KCZ. *Journal of Hydrology*: 125658. https://doi.org/10.1016/j.jhydrol.2020.125658

Medici, G., L.J. West, and S.A. Banwart. 2019a. Groundwater flow velocities in a fractured carbonate aquifer-type: Implications for contaminant transport. *Journal of Contaminant Hydrology* 222: 1–16.

Medici, G., L.J. West, P.J. Chapman, and S.A. Banwart. 2019b. Prediction of contaminant transport in fractured carbonate aquifer types: A case study of the Permian Magnesian Limestone Group (NE England, UK). *Environmental Science and Pollution Research* 26, no. 24: 24863–24884.

Medici, G., L.J. West, N.P. Mountney, and M. Welch. 2019c. Permeability of rock discontinuities and faults in the Triassic Sherwood Sandstone Group (UK): Insights for management of fluvio-aeolian aquifers worldwide. *Hydrogeology Journal* 27, no. 8: 2835–2855.

Medici, G., L.J. West, and N.P. Mountney. 2018. Characterization of a fluvial aquifer at a range of depths and scales: The Triassic St Bees Sandstone Formation, Cumbria, UK. *Hydrogeology Journal* 26, no. 2: 565–591.

Medici, G., L.J. West, and N.P. Mountney. 2016. Characterizing flow pathways in a sandstone aquifer: Tectonic vs sedimentary heterogeneities. *Journal of Contaminant Hydrology* 194: 36–58.

Mercuri, M., K.J. McCaffrey, L. Smeraglia, P. Mazzanti, C. Collettini, and E. Carminati. 2020. Complex geometry and kinematics of subsidiary faults within a carbonate-hosted relay ramp. *Journal of Structural Geology* 130: 103915.

Micarelli, L., A. Benedicto, and C.A.J. Wibberley. 2006. Structural evolution and permeability of normal fault zones in highly porous carbonate rocks. *Journal of Structural Geology* 28, no. 7: 1214–1227.

Miccadei, E., T. Piacentini, and G. Esposito. 2011. Geomorphosites and geotourism in the parks of the Abruzzo region (central Italy). *Geoheritage* 3: 233–251.

Mohamed, E.A., and R.H. Worden. 2006. Groundwater compartmentalisation: A geochemical analysis of the structural controls on the subdivision of a major aquifer, the Sherwood Sandstone, Merseyside, UK. *Hydrology and Earth System Sciences* 10: 49–64.

Murphy, P.J., and S. Everett. 2013. The "gulfs" of Greenhow Hill, North Yorkshire, UK. *Cave and Karst Science* 40, no. 2: 87–91.

Murphy, M.A., and W.P. Burgess. 2006. Geometry, kinematics, and landscape characteristics of an active transtension zone, Karakoram fault system, southwest Tibet. *Journal of Structural Geology* 28, no. 2: 268–283.

Murphy, P.J. 2000. The karstification of the Permian strata east of Leeds. *Proceedings of the Yorkshire Geological Society* 5: 25–30.

Musgrove, M., B.G. Katz, L.S. Fahlquist, C.A. Crandall, and R.J. Lindgren. 2014. Factors affecting public-supply well vulnerability in two karst aquifers. *Groundwater* 52: 63–75.

Neymeyer, A.R.T., P.L. Williams, and P.J. Younger. 2007. Migration of polluted mine water in a public supply aquifer. *Quarterly Journal of Engineering Geology and Hydrogeology* 40: 75–84.

Neuman, S.P. 2005. Trends, prospects and challenges in quantifying flow and transport through fractured rocks. *Hydrogeology Journal* 13, no. 1: 124–147.

Odling, N.E., L.J. West, S. Hartmann, and A. Kilpatrick. 2013. Fractional flow in fractured chalk: A flow and tracer test revisited. *Journal of Contaminant Hydrology* 147: 96–111.

Odling, N.E., P. Gillespie, B. Bourgine, C. Castaing, J.P. Chiles, N.P. Christensen, E. Fillion, A. Genter, C. Olsen, L. Thrane, and R. Trice. 1999. Variations in fracture system geometry and their implications for fluid flow in fractures hydrocarbon reservoirs. *Petroleum Geoscience* 5, no. 4: 373–384.

Odling, N.E., and J.E. Roden. 1997. Contaminant transport in fractured rocks with significant matrix permeability, using natural fracture geometries. *Journal of Contaminant Hydrology* 27: 263–283.

Odonne, F., C. Lézin, G. Massonnat, and G. Escadeillas. 2007. The relationship between joint aperture, spacing distribution, vertical dimension and carbonate stratification: An example from the Kimmeridgian limestones of Pointe-du-Chay (France). *Journal of Structural Geology* 29, no. 5: 746–758.

Ortiz, R.A.E., M. Dussel, and I. Moeck. 2018. Borehole geophysical characterisation of a major fault zone in the geothermal Unterhaching Gt 2 well, South German Molasse Basin. *Zeitschrift der Deutschen Gesellschaft für Geowissenschaften* 169, no. 3: 445–463.

Paillet, F.L. 1998. Flow modeling and permeability estimation using borehole flow logs in heterogeneous fractured formations. *Water Resources Research* 34, no. 5: 997–1010.

Panza, E., F. Agosta, M. Zambrano, E. Tondi, G. Prosser, M. Giorgioni, and J.M. Janiseck. 2015. Structural architecture and discrete fracture network modelling of layered fractured carbonates (Altamura Fm., Italy). *Italian Journal of Geosciences* 134, no. 3: 409–422.

Parker, B.L., K. Bairos, C.H. Maldaner, S.W. Chapman, C.M. Turner, L.S. Burns, J. Plett, R. Carter, and J.A. Cherry. 2019. Metolachlor dense non-aqueous phase liquid source conditions and plume attenuation in a dolostone water supply aquifer. *Geological Society of London Special Publications* 479: 207–236.

Parker, B.L., S.W. Chapman, and M.A. Guilbeault. 2008. Plume persistence caused by back diffusion from thin clay layers in a sand aquifer following TCE source-zone hydraulic isolation. *Journal of Contaminant Hydrology* 102: 86–104.

Parra, J., and X. Emery. 2013. Geostatistics applied to cross-well reflection seismic for imaging carbonate aquifers. *Journal of Applied Geophysics* 92: 68–75.

Parra, J.O., C.L. Hackert, and M.W. Bennett. 2006. Permeability and porosity images based on *P*-wave surface seismic data: Application to a south Florida aquifer. *Water Resources Research* 42. https://doi.org/10.1029/2005WR004114

Pepe, M., and M. Parise. 2014. Structural control on development of karst landscape in the Salento Peninsula (Apulia, SE Italy). *Acta Carsologica* 43, no. 1. https://doi.org/10.3986/ac.v43i1.643

Petitta, M., L. Mastrorillo, E. Preziosi, F. Banzato, M.D. Barberio, A. Billi, C. Cambi, G. De Luca, G. Di Carlo, D. Di Curzio, and C. Di Salvo. 2018. Water-table and discharge changes associated with the 2016–2017 seismic sequence in central Italy: Hydrogeological data and a conceptual model for fractured carbonate aquifers. *Hydrogeology Journal* 26, no. 4: 1009–1026.

Petitta, M., D. Fracchiolla, R. Aravena, and M. Barbieri. 2009. Application of isotopic and geochemical tools for the evaluation of nitrogen cycling in an agricultural basin, the Fucino Plain, Central Italy. *Journal of Hydrology* 372: 124–135.

Petitta, M., and M. Tallini. 2002. Idrodinamica sotterranea del massiccio del Gran Sasso (Abruzzo): nuove indagini idrologiche, idrogeologiche e idrochimiche (1994–2001). *Bollettino della Società' Geologica Italiana* 121: 343–363.

Petrella, E., P. Capuano, M. Carcione, and F. Celico. 2009. A high-altitude temporary spring in a compartmentalized carbonate aquifer: The role of low-permeability faults and karst conduits. *Hydrological Processes* 23, no. 23: 3354–3364.

Pollock, D.W. 1994. User's guide for MODPATH/MODPATH-PLOT, version 3: A particle tracking post-processing package for MODFLOW, the U.S. Geological Survey finite-difference ground-water flow model. U.S. Geological Survey, Open-File Report 94-464.

Reimann, T., C. Rehrl, W.B. Shoemaker, T. Geyer, and S. Birk. 2011. The significance of turbulent flow representation in single-continuum models. *Water Resources Research* 47, no. 9. https://doi.org/10.1029/2010WR010133

Reimann, T., and M.E. Hill. 2009. MODFLOW-CFP: A new conduit flow process for MODFLOW−2005. *Groundwater* 47, no. 3: 321–325.

Ritzi, R.W. Jr., and R.H. Andolsek. 1992. Relation between anisotropic transmissivity and azimuthal resistivity surveys in shallow, fractured, carbonate flow systems. *Groundwater* 30, no. 5: 774–780.

Rutqvist, J., C. Leung, A. Hoch, Y. Wang, and Z. Wang. 2013. Linked multicontinuum and crack tensor approach for modeling of coupled geomechanics, fluid flow and transport in fractured rock. *Journal of Rock Mechanics and Geotechnical Engineering* 5: 18–31.

Saller, S.P., M.J. Ronayne, and A.J. Long. 2013. Comparison of a karst groundwater model with and without discrete conduit flow. *Hydrogeology Journal* 21, no. 7: 1555–1566.

Santantonio, M., S. Fabbi, and S. Bigi. 2017. Discussion on "Geological map of the partially dolomitized Jurassic succession exposed in the central sector of the Montagna dei Fiori Anticline, Central Apennines, Italy" by G. Storti, F. Balsamo & A. Koopman. *Italian Journal of Geosciences* 136, no. 2: 312–316.

Sauro, F., D. Zampieri, and M. Filipponi. 2013. Development of a deep karst system within a transpressional structure of the Dolomites in north-east Italy. *Geomorphology* 184: 51–63.

Scozzafava, M., and M. Tallini. 2001. Net infiltration in the Gran Sasso Massif of central Italy using the Thornthwaite water budget and curve-number method. *Hydrogeology Journal* 9, no. 5: 461–475.

Selroos, J.O., D.D. Walker, A. Ström, B. Gylling, and S. Follin. 2002. Comparison of alternative modelling approaches for groundwater flow in fractured rock. *Journal of Hydrology* 257: 174–188.

Shoemaker, B.W., E.L. Kuniansky, S. Birk, S. Bauer, and E.D. Swain. 2008 Documentation of a conduit flow process (CFP) for MODFLOW-2005. Techniques and methods. U.S Geological Survey, Techniques and Methods Report Book 6, Chapter 6 A-24.

Smeraglia, L., O. Fabbri, F. Choulet, M. Buatier, P. Boulvais, S.M. Bernasconi, and F. Castorina. 2020. Syntectonic fluid flow and deformation mechanisms within the frontal thrust of foreland fold-and-thrust belt: Example from the Internal Jura, Eastern France. *Tectonophysics* 778: 228178.

Smeraglia, L., S.M. Bernasconi, F. Berra, A. Billi, C. Boschi, A. Caracausi, E. Carminati, F. Castorina, C. Doglioni, F. Italiano, and A.L. Rizzo. 2018. Crustal-scale fluid circulation and co-seismic shallow comb-veining along the longest normal fault of the central Apennines, Italy. *Earth and Planetary Science Letters* 498: 152–168.

Smeraglia, L., L. Aldega, A. Billi, E. Carminati, and C. Doglioni. 2016a. Phyllosilicate injection along carbonate-hosted extensional faults and implications for seismic slip propagation: Case studies from the central Apennines, Italy. *Journal of Structural Geology* 93: 29–50.

Smeraglia, L., F. Berra, A. Billi, C. Boschi, E. Carminati, and C. Doglioni. 2016b. Origin and role of fluids involved in the seismic cycle of extensional faults in carbonate rocks. *Earth and Planetary Science Letters* 450: 292–305.

Soliva, R., and A. Benedicto. 2004. A linkage criterion for segmented normal faults. *Journal of Structural Geology* 26, no. 12: 2251–2267.

Solum, J.G., and B.A.H. Huisman. 2016. Toward the creation of models to predict static and dynamic fault-seal potential in carbonates. *Petroleum Geoscience* 2: 70–91.

Sullivan, T.P., Y. Gao, and T. Reimann. 2019. Nitrate transport in a karst aquifer: Numerical model development and source evaluation. *Journal of Hydrology* 573: 432–448.

Tanner, P.G. 1989. The flexural-slip mechanism. *Journal of Structural Geology* 11: 635–655.

Tavani, S., F. Stort, O. Lacombe, A. Corradetti, J.A. Muñoz, and S. Mazzoli. 2015. A review of deformation pattern templates in foreland basin systems and fold-and-thrust belts: Implications for the state of stress in the frontal regions of thrust wedges. *Earth-Science Reviews* 141: 82–104.

Tomassetti, L., L. Petracchini, M. Brandano, F. Trippetta, and A. Tomassi. 2018. Modeling lateral facies heterogeneity of an upper Oligocene carbonate ramp (Salento,

southern Italy). *Marine and Petroleum Geology* 96: 254–270.

Tondi, E., M. Antonellini, A. Aydin, L. Marchegiani, and G. Cello. 2006. The role of deformation bands, stylolites and sheared stylolites in fault development in carbonate grainstones of Majella Mountain, Italy. *Journal of Structural Geology* 28, no. 3: 376–391.

Torabi, A., J. Jimenez-Millan, r. Jimenez-Espomosa, F.J. Garcia-Torosta, I. Abad, and T.S.S. Ellingsen. 2020. Effect of mineral processes and deformation on the petrophysical properties of soft rocks during active faulting. *Minerals* 10: 444. https://doi.org/10.3390/min10050444

Torabi, A., M.U. Johannessen, and T.S.S. Ellingsen. 2019a. Fault Core thickness: Insights from siliciclastic and carbonate rocks. *Geofluids* 2019: 1–24. https://doi.org/10.1155/2019/2918673

Torabi, A., T.S.S. Ellingsen, M.U. Johannessen, B. Alaei, A. Rotevatn, and D. Chiarella. 2019b. Fault zone architecture and its scaling laws: Where does the damage zone start and stop? *Geological Society, London, Special Publications* 496: 99–124. https://doi.org/10.1144/SP496-2018-151

Trippetta, F., B.M. Carpenter, S. Mollo, M.M. Scuderi, P. Scarlato, and C. Collettini. 2017. Physical and transport property variations within carbonate-bearing fault zones: Insights from the Monte Maggio Fault (central Italy). *Geochemistry, Geophysics, Geosystems* 18, no. 11: 4027–4042.

Tsang, Y.W., and P.A. Witherspoon. 1983. The dependence of fracture mechanical and fluid flow properties on fracture roughness and sample size. *Journal of Geophysical Research: Solid Earth* 88: 2359–2366.

Vecsei, A., and D.G. Sanders. 1997. Sea-level highstand and lowstand shedding related to shelf margin aggradation and emersion, Upper Eocene-Oligocene of Maiella carbonate platform, Italy. *Sedimentary Geology* 112: 219–234.

Voeckler, H., and D.M. Allen. 2012. Estimating regional-scale fractured bedrock hydraulic conductivity using discrete fracture network (DFN) modeling. *Hydrogeology Journal* 20, no. 6: 1081–1100.

Wang, X., Q. Lei, L. Lonergan, H. Jourde, O. Gosselin, and J. Cosgrove. 2017. Heterogeneous fluid flow in fractured layered carbonates and its implication for generation of incipient karst. *Advances in Water Resources* 107: 502–516.

Wang, X., A. Jardani, H. Jourde, L. Lonergan, J. Cosgrove, O. Gosselin, and G. Massonnat. 2016. Characterisation of the transmissivity field of a fractured and karstic aquifer, southern France. *Advances in Water Resources* 87: 106–121.

West, L.J., and N.E. Odling. 2007. Characterization of a multi-layer aquifer using open well dilution tests. *Groundwater* 45: 74–84.

Woodcock, N.H., and K. Mort. 2008. Classification of fault breccias and related fault rocks. *Geological Magazine* 145, no. 3: 435–440.

Worthington S.R.H. 1991. Karst hydrogeology of the Canadian Rocky Mountains. PhD thesis, McMaster University, Hamilton, Ontario.

Worthington, S.R. 2015. Diagnostic tests for conceptualizing transport in bedrock aquifers. *Journal of Hydrology* 529: 365–372.

Worthington, S.R., and D.C. Ford. 2009. Self-organized permeability in carbonate aquifers. *Groundwater* 47: 326–336.

Worthington, S.R., and J. Gunn. 2009. Hydrogeology of carbonate aquifers: A short history. *Groundwater* 47, no. 3: 462–467.

Xu, Z., B.X. Hu, H. Davis, and J. Cao. 2015. Simulating long term nitrate-N contamination processes in the Woodville Karst Plain using CFPv2 with UMT3D. *Journal of Hydrology* 524: 72–88.

Yager, R.M., C.I. Voss, and S. Southworth. 2009. Comparison of alternative representations of hydraulic-conductivity anisotropy in folded fractured-sedimentary rock: Modeling groundwater flow in the Shenandoah Valley (USA). *Hydrogeology Journal* 17, no. 5: 1111–1131.

Zambrano, M., E. Tondi, I. Korneva, E. Panza, F. Agosta, J.M. Janiseck, and M. Giorgioni. 2016. Fracture properties analysis and discrete fracture network modelling of faulted tight limestones, Murge Plateau, Italy. *Italian Journal of Geosciences* 135: 55–67.

Zhang, Y., Y. Zhang, Z. Kuang, J. Xu, C. Li, Y. Li, Y. Jiang, and J. Xie. 2019. Comparison of microbiomes and resistomes in two Karst groundwater sites in Chongqing, China. *Groundwater* 57, no. 5: 807–818.

Zuffianò, L.E., A. Basso, D. Casarano, V. Dragone, P.P. Limoni, A. Romanazzi, F. Santaloia, and M. Polemio. 2016. Coastal hydrogeological system of Mar Piccolo (Taranto, Italy). *Environmental Science and Pollution Research* 23, no. 13: 12502–12514.